THE DEVELOPMENT OF CALCIUM CARBONATE - IRON OXIDE PROTECTIVE COATINGS ON IRON

By

Mahmoud O. Abdullah

AN ABSTRACT

Submitted to the College of Graduate Studies of Michigan State University of Agriculture and Applied Science in partial fulfillment of the requirements for the degree of

Doctor of Philosophy

Department of Chemical Engineering

1958

Approved 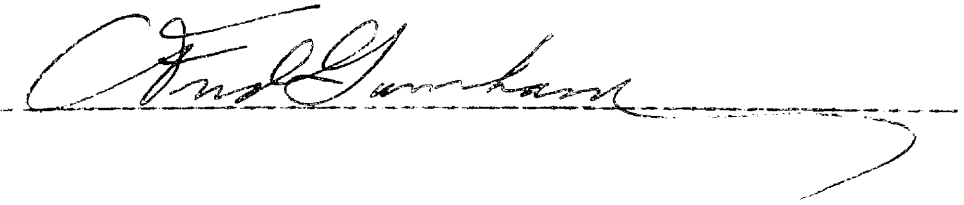

THE DEVELOPMENT OF CALCIUM CARBONATE - IRON OXIDE PROTECTIVE COATINGS ON IRON

ABSTRACT

The development of useful protective coatings for prevention of corrosion in water systems has been under investigation using both static and dynamic tests. All work has been with water containing calcium hydroxide, carbon dioxide, oxygen, and nitrogen.

Review of the literature indicated that a good understanding of the effects of pH, temperature, salinity, and other factors on the equilibrium of calcium carbonate in water has been reached. However the nature of the scale and the factors influencing its formation have not been completely established.

It has been the object of this research project to develop uniform coatings in a dense impermeable form that will provide high anti-corrosion protection, and to investigate and evaluate the effect of certain physical and chemical environmental conditions on the formation of these coatings.

Petrographic methods were used to identify the minerals developed on the specimens. Coating materials developed on cast iron specimens were largely limonite. Five to forty percent calcite was commonly present. Siderite and

magnetite were usually observed covered by limonite. With stainless steel specimens, only calcite was found.

Polarization studies indicated that $CaCO_3$ acted primarily as a cathodic inhibitor. The action of calcium carbonate in developing good protective films seemed to lie in forming a physical mixture with corrosion products. Under favorable conditions the mixture bonded well to the cast iron specimens and was hard and relatively tough.

Better protection and better bonded, harder, and tougher coatings resulted from solutions containing colloidal $CaCO_3$ than from identical solutions of the same pH and hardness with no colloids present. Colloidal $CaCO_3$ was found to have a positive charge in the pH range 6 - 11 and may be represented as $(CaCO_3)\ Ca^{++}|OH^-$. Calcium carbonate crystals in suspension did not have a favorable effect on formation of coatings from supersaturated solutions.

Relatively high flow velocities of about 2 feet per second were desirable in the formation of hard durable coatings. Static tests generally produced soft coatings. A saturated level of oxygen was found to be optimum for developing good coatings under the conditions conducted in this study.

A high momentary excess of $CaCO_3$ led to the formation of chalky soft coatings. Low momentary excesses and high saturation excesses of $CaCO_3$ led to the formation of hard,

tough, protective coatings.

Thus, it has been established that when a water is saturated with dissolved oxygen, is of pH 8.2 to 8.7, contains a momentary excess of 2.5 to 5.5 ppm $CaCO_3$ in the presence of colloidal $CaCO_3$, and flows at a velocity of about two feet per second, a uniform, hard and well bonded coating can be developed on cast iron specimens in one day's time at room temperature.

THE DEVELOPMENT OF CALCIUM CARBONATE - IRON OXIDE PROTECTIVE COATINGS ON IRON

By

Mahmoud O. Abdullah

A THESIS

Submitted to the College of Graduate Studies of Michigan State University of Agriculture and Applied Science in partial fulfillment of the requirements for the degree of

Doctor of Philosophy

Department of Chemical Engineering

1958

Approved_____

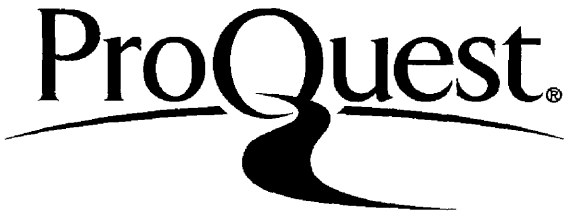

ACKNOWLEDGMENT

This thesis was only possible with the sincerely appreciated support of a N.I.H. grant.

The author wishes to express his sincere appreciation to Dr. R.F. McCauley and Dr. C.F. Gurnham for their valuable guidance and assistance in connection with this thesis.

Thanks are also extended to Dr. H. Stonehouse and Mr. C. Star for their help in the analyses of the coatings developed.

TABLE OF CONTENTS

Page

LIST OF FIGURES

Figure Page

LIST OF TABLES

INTRODUCTION

All water systems undergo corrosion, generally at slow but continuous rates. In some systems waters are so "aggressive" as to seriously damage pipes and appurtenances within a few years. In other instances, tuberculation continues over long periods, gradually decreasing the carrying capacity of the system and resulting in various degrees of "red water." Losses from corrosion are of major importance in both municipal and industrial water works. In addition to direct economic losses, the water works industry suffers from over-design of structures in anticipation of corrosion, reduced capacities of pipelines, increased hazard of structural failure during peak or fire demands, and impairment of water quality by corrosion products entering solution.

For these reasons the development of means for reducing corrosion in water systems is of prime importance. Natural protective coatings, usually of calcium carbonate or mixtures of calcium carbonate and corrosion products, are now widely used in water works practice for prevention of excessive corrosion and for overcoming "red water" problems. No satisfactory procedure so far exists, however, for developing satisfactory protective coatings under all normal operating conditions. Coatings are in some instances dense, hard, and

uniform; while in other instances they are soft, rough, and permeable.

It has been the object of this thesis to learn how the coatings can be uniformly laid down in a dense impermeable form that provides high anti-corrosion protection without damage to hot and cold distribution systems. To accomplish the objectives of this thesis problem, the mechanism of laying down these desirable protective coatings has been studied and an investigation of the effect of certain physical and chemical environmental conditions on their formation has been made. Petrographic methods have been used to identify the materials which formed the scales under various conditions.

LITERATURE REVIEW

Anhydrous calcium carbonate occurs in nature in at least three known forms under various conditions of precipitation (1). Of these three forms, rhombohedral or calcite is the most stable at ordinary temperatures. Orthorhombic aragonite is only slightly stable and, in water, tends to transform into calcite at an extremely low rate at ordinary temperatures and pressures. The third form, vaterite, is unstable and changes into either aragonite or calcite.

The early use of calcium carbonate scale for inhibiting corrosion was necessarily on an empirical basis. In time, practical and useful tests (such as the marble test by Tillmans and collaborators (2)) were developed to determine the degree of supersaturation or undersaturation of a water. These methods helped to predict the tendency toward deposition or removal of scale.

The development of the "saturation index" by Langelier (3) was based upon principles of physical chemistry which will be dealt with later under theoretical considerations. The "saturation index" is the measure of the driving force tending to bring a water to stability. A positive index indicates that scale will be laid down, a negative index that scale will be dissolved. A water may be adjusted to a

positive scale forming index by adding lime and/or sodium carbonate. Such adjustment is easily accomplished by methods suggested by Moore (4) and others. Enslow (5) has devised a "continuous stability indicator" to measure the degree of supersaturation or undersaturation of a water.

Refinements in computation of the "saturation index" have resulted from further studies by Langelier (6) and others. McKinney (7) has discussed the calculation of equilibria in dilute water solutions and has pointed out the effect of alkalinity on changes in pH that might be expected due to temperature increases. Larson and Buswell (8) have discussed the effect of salinity on ionization constants, thus increasing accuracy in determining "saturation indexes" at different temperatures.

Ryznar (9) has proposed an empirical "stability index," which will also be discussed later under theoretical considerations, with a view to providing an indication of the degree of scaling that can be anticipated. It has also been suggested by Dye (10) and others that the deficit or excess of carbon dioxide in a given alkalinity-calcium-pH system might be used as an index of scaling.

From the preceding information it can be seen that a good understanding of the effect of pH, temperature, salinity, and other factors upon the equilibrium of calcium carbonate in water has been reached. However, the nature of the scale

and the manner in which it is formed are far from being completely understood at the present time.

It has been shown by Larson and King (11), Raistrick (12), and Evan (13) that calcium carbonate can be deposited from calcium bicarbonate solution in an electrochemical process at the cathode. The precipitated calcium carbonate is directly proportional to the current density.

According to Evan (14) and Haase (15), a heterogeneous layer of rust and calcium carbonate gives a better protection from corrosive attack than does a layer of rust alone or a layer of calcium carbonate alone.

Evan (14) has expressed the opinion that rusting iron yields ferrous oxide or hydroxide which is then oxidized to the less soluble ferric oxide. Additional ferrous oxide then diffuses outward through the ferric oxide and iron continues to move into solution in spite of the coating of ferric oxide. Calcium carbonate in the presence of oxygen interacts with iron salts to form a clinging ferric oxide rust. If oxygen is present in large amounts, the rust is formed very close to the metal and ferrous salts and calcium carbonate interact to yield ferrous carbonate which is then oxidized. In the absence of oxygen, magnetite appears; this is loose and not protective.

The data of Strum (16) on cast iron specimens exposed to oxygen-saturated water of varying hardness and pH

indicates that a high proportion of calcium carbonate in the film is more desirable in retarding corrosion than an increase in film thickness. Coatings developed were found to contain a much higher percentage of calcium carbonate in the layers closest to the iron surface than the exterior layers which were predominately iron oxide.

Baylis (17) has shown that ferrous carbonate is produced in varying quantities as a product of corrosion if the carbonic acid is present either as free or half-bound carbon dioxide (CO_2 and HCO_3^-). Reaction takes place either directly with metallic iron or with iron oxides or hydroxides. Baylis' tests also showed that ferrous carbonate in the absence of oxygen is practically insoluble at a pH and alkalinity close to the calcium carbonate saturation curve, but that the solubility increases very rapidly if the pH is decreased below the level necessary for calcium carbonate equilibrium. Baylis has stated that ferrous carbonate aids in protecting iron surfaces where the pH and alkalinity are above calcium carbonate equilibrium, especially if the ferrous carbonate is overlaid by some kind of a coating that protects it from dissolved oxygen.

The relationship between the formation of coatings and the dissolved oxygen level in water has not been completely established. American water works practice is generally to reduce dissolved oxygen to the minimum possible level since

oxygen is the primary factor controlling the corrosion rate. On the other hand, European workers, as reviewed by Evan (14), intentionally aerate the water before it enters the pipe line so that the dissolved oxygen concentration will be increased. Their argument is that corrosion resulting from the oxygen content of the water is desirable for promoting and accelerating deposition of a calcium carbonate protective coating on the metal. According to Schikorr (18), Haupt (19), and others, an oxygen concentration of at least 6 mg per liter is necessary to produce a protective coating.

Camp (20) in his thermodynamic treatment of an electrochemical corrosion has shown that ferrous hydroxide, $Fe(OH)_2$, will not form on iron unless the pH value of the solution exceeds 9.

Evan (14) has reviewed the work of a number of authors who have reported on different species of rust developed in electrochemical corrosion. Quoting Schikorr (21), Evan has stated that the oxidation of ferrous hydroxide to hydrated ferric oxide FeO(OH) results in goethite if the oxidation is rapid and produces the mineral lepidocrocite if slow oxidation takes place. In the formation of lepidocrocite, a ferrous-ferrite material is first developed which in turn yields the hydrated ferric oxide.

Girard (22) has suggested that ferrous hydroxide is

first formed on the metal face of corroding iron and that exposure to oxygen changes the deposit to the ferric condition. The ferric material in turn reacts with ferrous hydroxide to form green hydrated magnetite, $Fe_3O_4 \cdot H_2O$ which acts as an intermediate body. The diffusion of oxygen to the green body yields either goethite or lepidocrocite. If oxygen is deficient, the green intermediate undergoes dehydration to black inert magnetite. Thus, stratified layers of different iron oxides are often formed in the electrochemical corrosion of iron.

THEORETICAL CONSIDERATIONS

A. Electrochemical Theory of Corrosion of Iron

The electrochemical theory of corrosion proposed in 1903 by W. R. Whitney (23) has been widely accepted by students of this phenomena. The theory has been discussed by many prominent authors in the field of corrosion, including Uhlig (24), Speller (25), Evan (14), Eliassen and co-workers (26), and others. The fundamental mechanisms involved in this theory can be described in the following manner:

1. The process of electrochemical corrosion requires the presence of anodic and cathodic areas. The anodic area (electronegative) is the area over which the metal is attacked (oxidized), and the cathodic area (electropositive) is that at which some substance from the environment is reduced. If the process is to continue, an electric current must flow between these areas through the environment (usually an aqueous solution) and between these areas in the metal. This electric current is carried by the electrons through the metal and is carried jointly by cations and anions, which migrate in opposite directions through the solution.

The combination of anode area, cathode area, and aqueous solution constitutes a small galvanic cell. Cells of this type may be set up on a single metallic surface or between dissimilar metals.

2. A flow of electricity results from the loss of two electrons from each iron atom leaving the crystal lattice of the metal as ferrous ion and entering the solution at the anode.

$$Fe^{o} = Fe^{++} + 2e \qquad (1)$$

3. Water partly dissociates into hydrogen ions and hydroxyl ions (one molecule in every 555,000,000 dissociates into its constituent H^{+} and OH^{-} ions)

$$H_2O = H^{+} + OH^{-} \qquad (2)$$

Ferrous ions react with hydroxyl ions to form ferrous hydroxide, $Fe(OH)_2$, which is soluble in water to the extent of 7.0 ppm at 20° C.

$$Fe^{++} + 2(OH)^{-} = Fe(OH)_2 \qquad (3)$$

In the presence of oxygen, ferrous hydroxide is oxidized to ferric hydroxide, $Fe(OH)_3$, or hydrous ferric oxide, commonly recognized as rust.

$$4Fe(OH)_2 + 2H_2O + O_2 = 4Fe(OH)_3 \qquad (4)$$

4. At the cathodic area the electrons are accepted by the hydrogen ions to form elementary hydrogen atoms.

$$2H^{+} + 2e = 2H^{o} \qquad (5)$$

This removal of hydrogen ions causes an increase in the concentration of hydroxyl ions in the area, and results in the production of alkaline conditions in the vicinity of the cathode.

5. If the hydrogen thus formed remains on the surface the area becomes polarized by the counter potential produced. This retards the flow of electrons and consequently the solution of iron.

6. In the majority of cases, however, the areas are depolarized, allowing the action to continue. Hadley (27) has enumerated five depolarization processes which may govern the rate of hydrogen removal from the cathode.

   a. Reaction of dissolved oxygen with nascent hydrogen to form water.

$$2H^{o} + \tfrac{1}{2}O_2 = H_2O \qquad (6)$$

   b. Agitation causing the removal or sweeping off of hydrogen as gas bubbles.

$$2H^{o} = H_2 \qquad (7)$$

   c. Direct chemical combination with electrolyte or salt. For instance, ferric ions may be reduced to ferrous ions by the hydrogen or by the electrons.

$$2Fe^{+++} + 2H^{o} = 2Fe^{++} + 2H^{+} \qquad (8)$$

$$2Fe^{+++} + 2e = 2Fe^{++} \qquad (9)$$

d. Reaction in the metabolic processes of certain anaerobic bacteria.

e. Combination with the products of microbiological metabolic processes.

The first two of the above processes are well known and may be observed in varying degrees in water corrosion processes. In acid solutions, usually of pH below 5, cathodic film is removed mainly as bubbles of gas. The hydrogen ion pressure is sufficient to overcome the hydrogen overvoltage at the metal surface, causing marked evolution of hydrogen gas. This accounts directly for the fact that corrosion is generally more rapid in acid solutions and less rapid in alkaline solutions. In neutral or alkaline solutions, the amount of gaseous hydrogen is very small compared with the amount of hydrogen destroyed by oxidation. Thus, in the pH range commonly encountered in natural waters, destruction of the hydrogen film is mainly governed by depolarization with dissolved oxygen. Since the cathodic reaction controls the rate of corrosion process, as will be explained later in this section, the depolarization reaction and, therefore, the rate of oxygen supply to the cathodic regions of the iron surface is the factor governing the rate

of corrosion in natural waters.

B. Typical Corrosion Cell on the Surface of Submerged Iron

Figure I shows schematically a typical corrosion cell on the surface of a submerged piece of iron. The anode and cathode of this cell are short circuited by the body of the metal. The surface of a large section of metal might be covered by many such corrosion cells. Formation of anodes and cathodes on a submerged metal are due mainly to (20, 26):

a. Difference in metal composition,

b. Difference in electrolyte concentrations (forming concentration cells),

c. Difference in aeration (the portion of the metal that has freer access to oxygen acts as the cathode, while the portion shielded from oxygen becomes the anode of the differential aeration cell), and

d. Difference in temperatures or stresses.

In the corrosion cell shown in Figure I, iron passes into solution at the anode area leaving electrons on the metal. These electrons pass through the metal to the cathode area, where they may be removed from the iron through reaction with hydrogen ions in solution producing atomic hydrogen (Equation 5), or by one of many other half-cell reactions which depend on the substances present in the

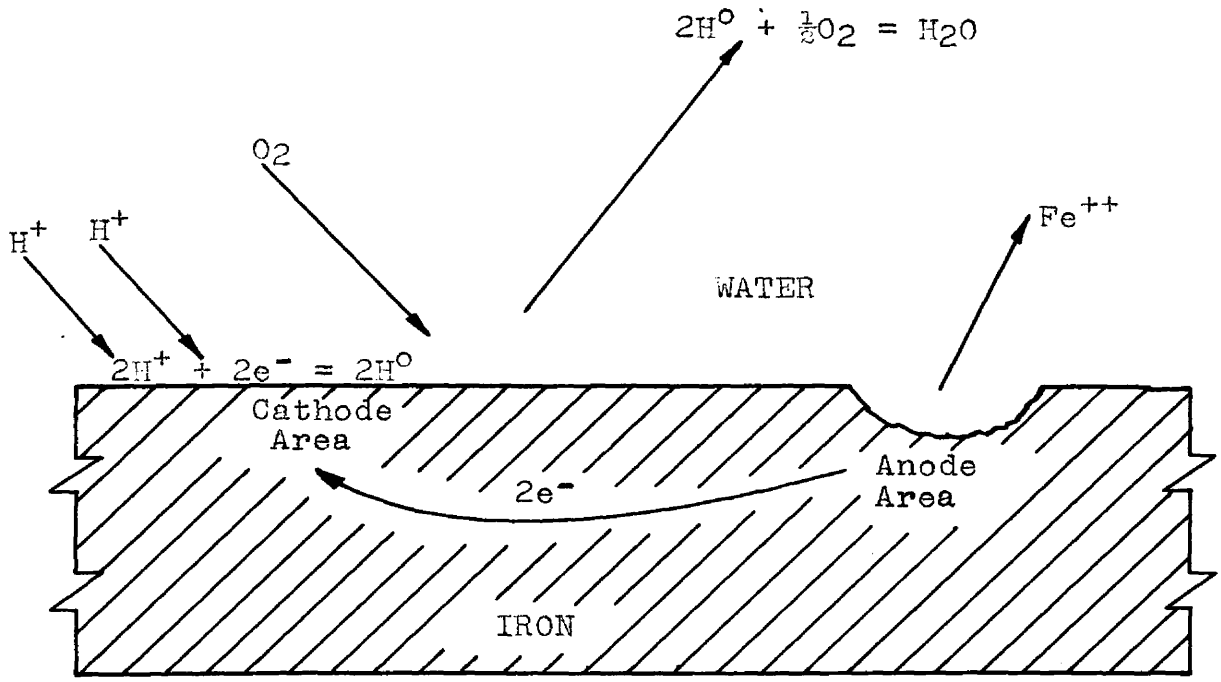

Figure 1 - Corrosion Cell on Surface of Submerged Iron

vicinity of the cathode and the relative energies governing half-cell reactions (26). Under certain conditions the hydrogen atoms tend to plate out on the metal and unless removed will interfere with transfer of other electrons to solution. Within the pH range normally encountered in water works practice, it is generally considered, that removal of hydrogen film from the cathode is by oxygen depolarization (Equation 6).

Wilson (28) has pointed out that anode reaction rate (Equation 1) is much faster than the depolarization reaction rate at the cathode (Equation 6 or 7). It is obvious that if a process comprises two or more separate reactions, the rate of the process as a whole is determined by the rate of the slowest of these reactions under the particular conditions. This is illustrated by the fact that though in the case of iron an increase in the metal-ion concentration should lessen the rate of anode reaction (Equation 1), it is without appreciable effect on the over-all rate of corrosion. Thus, cathodic reactions, govern the rate of corrosion process.

C. The Action of Inhibitors

Speller (25) has defined an inhibitor as a chemical substance or mixture which, when added to an environment,

usually in small concentration, effectively decreases corrosion. The protective action of inhibitors is due mainly to the formation of films on the metal surface. These films in turn retard the corrosion reactions. Film formation may occur preferentially at either anodes or cathodes of corrosion cells, or it may be adsorbed generally over the entire surface of the metal. Evan (14) has classified inhibitors into three classes:

(1) Anodic inhibitors

(2) Cathodic inhibitors

(3) Adsorption inhibitors

It should be noted that these classes are not clearly defined since some inhibitors may act in more than one way (26).

Anode films may be formed through electrodeposition of negatively charged ions or colloidal particles on this electrode, through adsorption of chemicals on the metal surface, or through the production of an insoluble precipitate by reaction between the iron entering solution and chemicals in solution. Anodic inhibitors reduce the rate of corrosion by restraining anodic reaction. The addition of a sufficient quantity of anodic inhibitor to a water could result in the formation of a continuous film over the anode areas which would be effectively separated from the water, thus stifling the anode reaction.

Although anodic inhibitors are very effective in reducing the over-all rate of corrosion, they are somewhat undesirable and even dangerous. As Evan (14) has pointed out, these inhibitors may intensify corrosion if used unwisely. Addition of insufficient anodic inhibitor to the corrosive medium would result in the formation of only partially protective film over the anode areas. It has been pointed out previously that the rate of corrosion of iron in water is generally governed by the rate at which cathodic reactions take place. Therefore, partial covering of the anodes has little effect on the over-all rate at which metal passes into solution, and may result in intensification of attack on the smaller remaining anodic areas with rapid failure of the structure by pitting. The use of anodic inhibitors in municipal water systems, therefore, would require the closest possible expert control.

Cathodic films may result from the electrodeposition of positively charged ions or colloidal particles on the cathode, from adsorption of chemicals on the metal surface, or from the insoluble precipitates formed on the metal by a reaction between chemicals in solution and the alkalinity produced at this electrode. Cathodic inhibitors reduce the rate of corrosion by interfering with cathodic reactions. These inhibitors, when used in proper concentrations (24), are less effective in reducing the over-all corrosion rate

than anodic inhibitors, due in part to the fact that a protective film is formed on the cathode. The film sets up a differential aeration cell, with the shielded cathode tending to become anodic to the exposed anode. This results in continual changes in the locations of anodes and cathodes while corrosion continues at a reduced rate (26).

The protective film formed by a cathode inhibitor interferes with the access of dissolved oxygen to the metal surface, and reduces the effective area of the cathode. Any reduction in the effective cathodic area must result in a corresponding reduction in the over-all corrosion rate. Cathodic inhibitors always render the corrosion less intense, even if they do not completely arrest the loss of metal. If a cathodic inhibitor is added in an amount sufficient to stop corrosion, the decrease in cathodic reaction permits an extension of the anodic areas, and helps to make corrosion less intense (14). Thus, the intensity of corrosion is diminished, under cathodic control, by reducing the total corrosion and by increasing the area over which the attack is spread. Contrary to the use of an anodic inhibitor, miscalculation in the amount of chemicals required will not lead to intense attack at some point with a resulting failure of the structure. For this reason Evan (14) has classified cathodic inhibitors as safe.

Some organic substances appear to be adsorbed over the

entire metallic surface (14). These compounds may be classed as adsorption inhibitors, and may interfere with either or both electrode reactions.

D. Polarization and the Rate of Corrosion

The action of corrosion inhibitors may be illustrated through polarization studies of either or both electrodes (14, 24, 25, 26). It has been stated previously that, for the process of corrosion to continue, an electric current must flow between different areas of the metal surface. In general, when current flows between two electrodes, a special opposition to current flow develops at the surface of the electrodes. This special opposition to current flow is termed polarization. Polarization of the electrode from which positive electricity leaves to enter the electrolyte (the anode) is termed anodic polarization, and that of the electrode to which positive electricity from the solution flows (the cathode) is termed cathodic polarization. The effect of both types of polarization is to reduce the effective difference in potential between the local anodes and local cathodes. Thus, polarization reduces current flow and consequently retards corrosion.

Figure 2 shows a typical pair of polarization curves, indicating the potentials of the anode and cathode of a

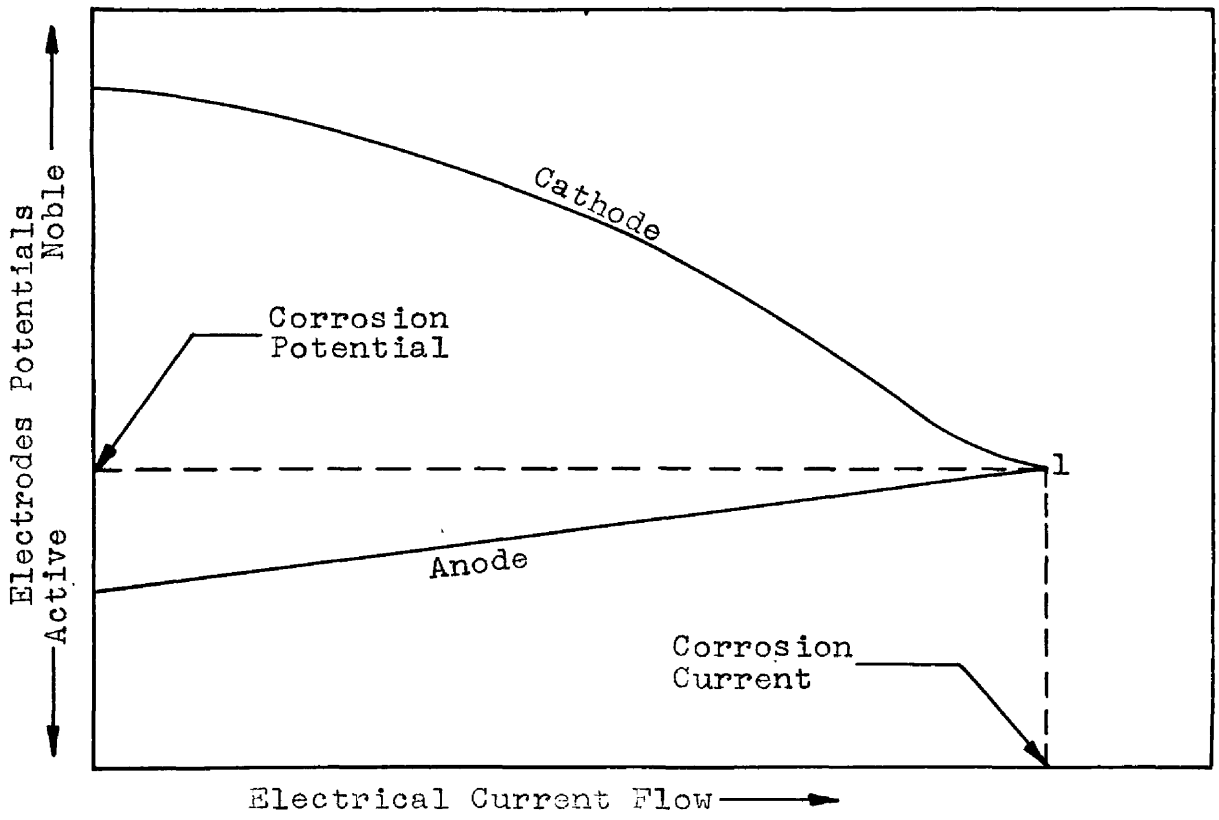

Figure 2 - Typical Polarization Curves

corrosion cell at various values of current flow between the electrodes. The points at which the curves intercept the ordinate axis represent the open circuit potentials of the electrodes (no current flowing in the corrosion cell). As the current flow through a corrosion cell increases, the potentials of the anode and cathode tend to approach a common value. Polarization of both electrodes would result in a shift in the anode potential in the cathodic direction and a shift in the cathode potential in the anodic direction. Therefore, the potential difference between the electrodes in a corrosion cell through which current is flowing is usually less than the difference in the open circuit potentials (or potentials of electrodes with no current flowing). The intersection of the curves at point 1 gives the corrosion potential and the corrosion current with the electrode short circuited, which is usually the situation in practice with both electrodes located on single piece of metal. It is to be noted that corrosion potential represented by point 1 of Figure 2 has been determined for most of the dynamic tests of this study in order to follow the action of the inhibitor with time under various conditions which will be discussed later.

The rate of corrosion can be controlled by the rate of the cathode reaction, the anode reaction, or both. Altogether, four types of control are possible in corrosion

cells. These are illustrated by Figure 3.

The addition of anodic inhibitor to a corrosion system results in increased polarization of the anode, as illustrated in Figure 3a. The increase in the degree of polarization is shown by an increase in slope of the anode line, indicating a greater change in anode potential for a given change in electrical current flow of the cell. In this case the corrosion is said to be under anodic control. The addition of the inhibitor results in a decrease in corrosion rate and a more noble corrosion potential.

The addition of cathodic inhibitor to a corrosion system causes an increased polarization of the cathode. Figure 3b represents the condition under cathodic control, resulting in corresponding reduction in current flow and corrosion rate, and a less noble corrosion potential.

Figure 3c shows polarization curves when the rate of corrosion is controlled by both electrodes (mixed control). Figure 3d represents the limiting case of resistance control, in which current flow between the electrodes has no effect on the potential of either of them. This situation would never occur in water works practice.

The addition of an inhibitor to a corrosion system may have an added effect on polarization curves by causing a change in the open-circuit potential of either or both electrodes.

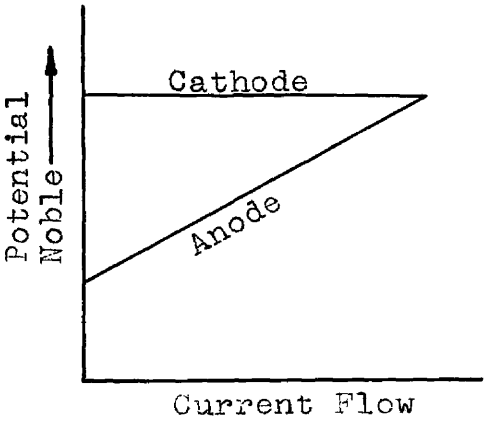

a - Anodic Control

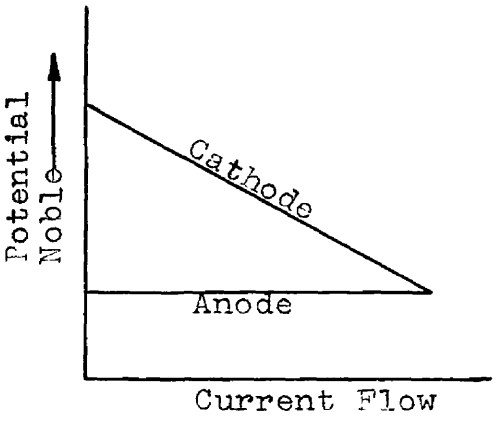

b - Cathodic Control

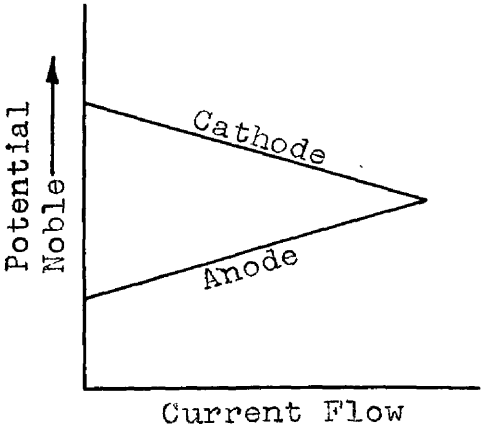

c - Mixed Control

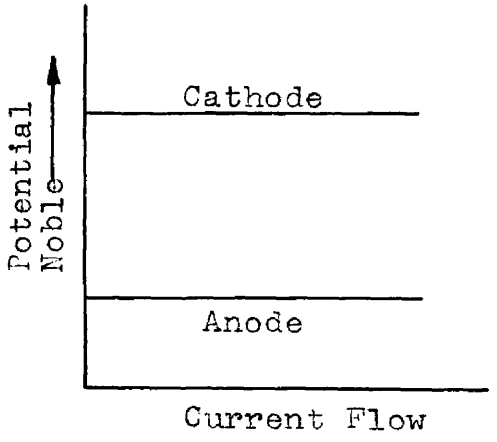

d - Resistance Control

Figure 3 - Types of Corrosion Control

In most municipal and industrial water systems, corrosion is primarily under cathodic control, as illustrated by Figure 3b. The rate of corrosion is governed by the degree of polarization of the cathode.

E. Different Indexes Used for Calcium Carbonate Equilibrium

1. Langelier Saturation Index

The basic reaction involved in the reversible pipe scaling process can be written:

$$CaCO_3 \text{ (solid)} + H^+ = Ca^{++} + HCO_3^- \qquad (10)$$

At equilibrium, therefore, the product of the molal concentrations of calcium and bicarbonate divided by the molal concentrations of hydrogen ion will remain constant, or

$$\frac{(Ca^{++})(HCO_3^-)}{(H^+)} = K \qquad (11)$$

Expressing each term as negative logarithms we can write for the pH at equilibrium

$$pH_{eq.} = pCa^{++} + pHCO_3^- - pK \qquad (13)$$

By formulating $pHCO_3^-$ in term of pH and total alkalinity at all pH levels and by showing that the -pK term of equation (12) is actually the difference between pK_2 (the ionization constant of the acid HCO_3^-) and pK_s (the solubility product constant for calcium carbonate), Langelier (3, 6) has developed the following expression for $pH_{eq.}$:

$$pH_s = (pK_2 - pK_s) + pCa^{++} + pAlk. + \log \; 1 + \frac{2K_2}{H_s} \qquad (13)$$

Where pK_2 and pK_s respectively, are the negative logarithms of the second ionization constant of carbonic acid and the solubility product constant of calcium carbonate, corrected for ion activity; pCa^{++} is the negative logarithm of the concentration of calcium ion in moles per liter; pAlk. is the negative logarithm of the titrable alkalinity in equivalents per liter; k_2 is the second ionization constant of carbonic acid; H_s is the hydrogen ion concentration at a hypothetical saturation with calcium carbonate; and pH_s is the pH value corresponding to the above hydrogen ion concentration, that is the pH at which a water of given calcium content and alkalinity is in equilibrium.

Langelier also introduced the "saturation index" which is the algebraic difference between the actual pH of a sample of water and calculated pH_s

Saturation index = pH actual - pH saturation

$$\text{Saturation index} = \log \frac{1}{(H^+)} - \log \frac{1}{(H_s^+)} = \log \frac{(H_s^+)}{(H^+)} \qquad (14)$$

Actually this index, as seen from equation (15), is the logarithm of the ratio of the hydrogen ion concentration which the sample must have if saturated (without change in composition) to its actual hydrogen ion concentration. If the index is zero the sample is in equilibrium.

A plus value for the saturation index indicates

oversaturation and a tendency to deposit $CaCO_3$; a minus value indicates undersaturation and a tendency to dissolve $CaCO_3$.

Saturation index varies with hot and cold water systems due to the difference in the rate of change of pH and the Langelier constant with temperature. A method for predicting this variation has been suggested by Powell, Bacon, and Lill (29). Dye (30) has also described a practical means for predicting pH values of a water at different temperatures.

Saturation index, according to Langelier, is an indication of directional tendency and of driving force, but it is not a measure of capacity. The amount of calcium carbonate deposited cannot be predicted from equilibrium data alone. Such deposition is dependent upon the relative rate of precipitation from solutions which are supersaturated with $CaCO_3$. $CaCO_3$ has a strong tendency to remain in supersaturated solution and in the absence of crystallization nuclei oversaturated calcium carbonate solutions can be preserved for years.

In general, more scale will be laid down at a low pH of saturation than a high pH of saturation. "Saturation index" is often of benefit to water chemists in determining whether waters are scale-forming or corrosive. Even in this respect "saturation index" is not always reliable,

because some waters with a positive index actually may be quite corrosive. This point has been observed and reported by Hoover (31) and others.

2. Ryznar Stability Index

Ryznar (9) has introduced an empirical expression, 2pHsaturation - pHactual, which he has designated "stability index", to differentiate it from Langelier's "saturation index." It has been claimed by Ryznar that "stability index" is not only an index of $CaCO_3$ saturation, but is also of quantitative significance. Unlike the "saturation index," the "stability index" is positive for all waters. Experimenting with the formation of calcium carbonate scale on glass coil at 120-200° F., Ryznar has found incrustation to take place within a two-hour test period at a stability index of 6 and below. No deposits have been obtained at an index value of above 7.5. Ryznar's "stability index" has been widely used in waterworks practice.

3. Saturation Excess

"Saturation excess" is the amount of calcium carbonate precipitation (in ppm) which must take place to bring a calcium-carbonate-bicarbonate-carbon dioxide system to equilibrium. It can be determined experimentally by the "marble" test, in which the water is placed in contact with

powdered $CaCO_3$. The decrease or increase in alkalinity is then a measure of "saturation excess" or "saturation deficiency". "Saturation excess" can also be determined graphically using methods developed by Langelier (6) and Dye (32).

4. Momentary Excess

Dye (32) has defined "momentary excess" as that fraction of calcium and carbonate ions present (in ppm $CaCO_3$) of an aqueous solution which is in excess of the solubility product constant of calcium carbonate. Dye also developed a graphical method for determining "momentary excess" based on the following equation:

$$(Ca^{++} - X)\ (CO_3^{=} - X) = K_s^{-}\ 10^{10} \qquad (16)$$

Where Ca^{++} and $CO_3^{=}$ are the initial concentrations of calcium and carbonate ions respectively, in terms of ppm of calcium carbonate; K_s^{-} is the solubility product constant for calcium carbonate corrected for temperature and dissolved solids; and X is the momentary excess in ppm of calcium carbonate. "Momentary excess" has been extensively used in the work reported in this thesis because it is a quantitative measure of the driving force tending toward calcium carbonate deposition.

EXPERIMENTAL APPARATUS AND MATERIAL

Work done on this project can be divided into two categories: (A) static tests and (B) dynamic tests.

A. Static Test Unit

Each static test was conducted in a glass cylinder eight inches in diameter and eighteen inches high as shown in Figure 5. To each cylinder fourteen liters of de-ionized water was added, filling the cylinder to within one inch of the top. Two specimens of cast iron or stainless steel were totally immersed in each cylinder by attaching each specimen to a glass rod by means of a nichrome wire and rubber band. The immersed portion of the nichrome wire was insulated by a waterproof rubber tape. The two glass rods with the specimens attached were fixed vertically in each cylinder so that the specimens were parallel, facing each other with a spacing of four inches. The water in the cylinders was stirred throughout each test by bubbling air continuously. The air supply was first passed through a cotton bed to remove particulate matter and then through a soda-lime bed to remove CO_2.

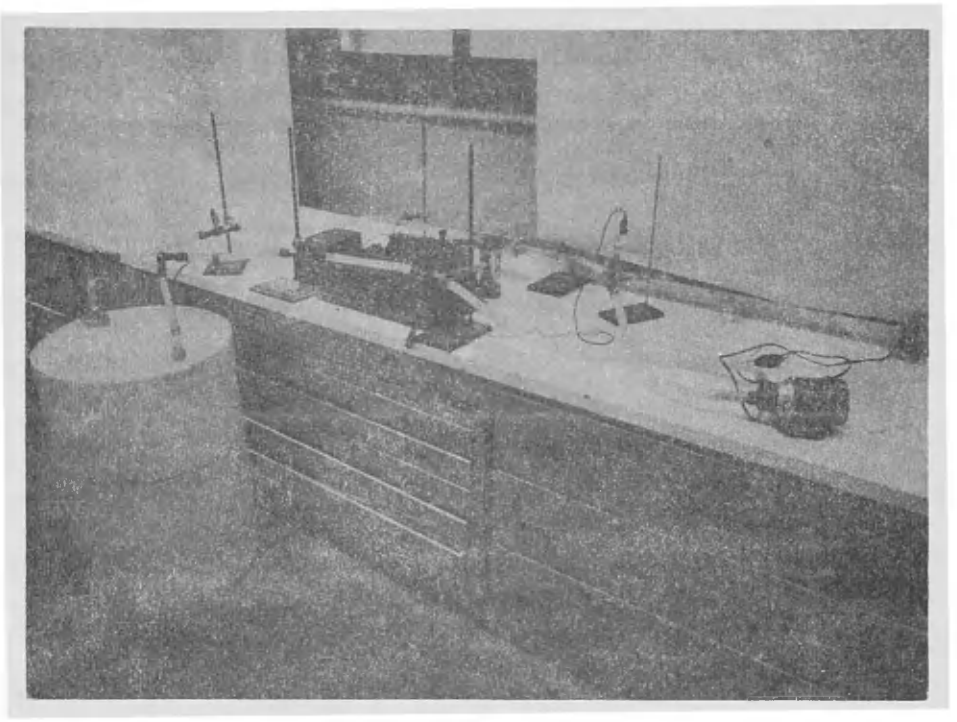

Figure 4.
Equipment for Dynamic Tests

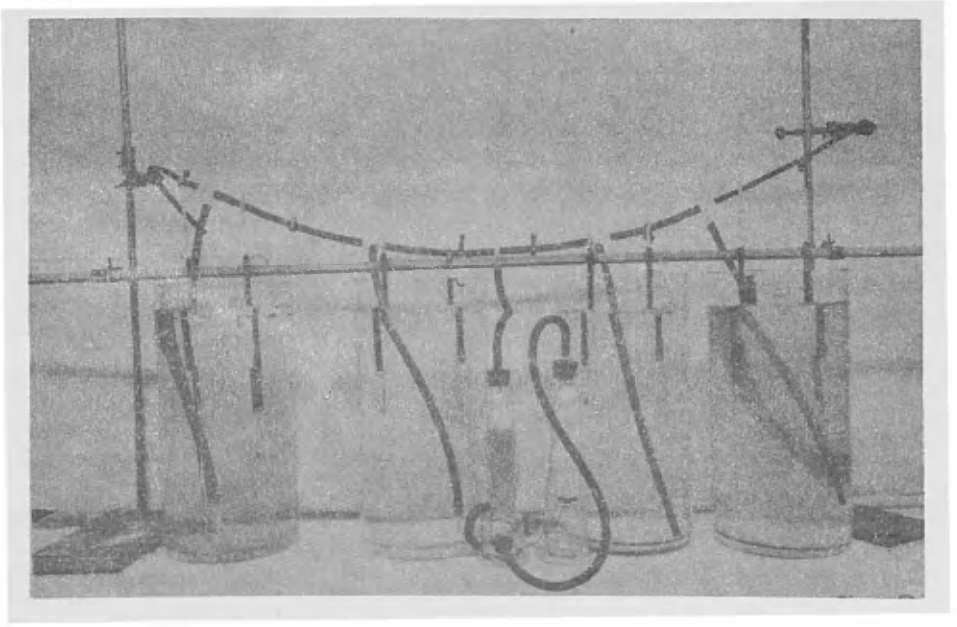

Figure 5.
Equipment for Static Tests

B. Dynamic Test Unit with Recirculated Water

Apparatus for dynamic tests with recirculated water is shown in Figures 4 and 6. A fifty-five gallon polyethylene barrel was used as reservoir for the water, which was circulated through the test cell by an all-rubber Universal Electric Company centrifugal pump. All parts of the pump in contact with the liquid were Hycar (synthetic rubber).

Construction of the test cell is shown in Figure 7. The cell was built of Lucite plastic to act as a housing for two metal specimens and to allow measurement of their potentials. A 3/4-inch hole was bored through the central axis and two parallel slots were machined, each at a distance of 1/4 inch from the center. The two specimens were mounted parallel in the cell through the slots, separated by a distance of 1/2 inch, in order to permit water flow parallel to their surfaces. Holes were drilled and tapped on either side of the cell to connect each specimen with a platinum wire for potential measurements. Tapered Lucite inserts were used to reduce turbulence in the vicinity of the specimens, the width and thickness of the inserts being the same as that of the specimens.

In some tests, where only one specimen was used, the test cell was of similar construction with only one slot located at the center of the 3/4-inch hole. One side only

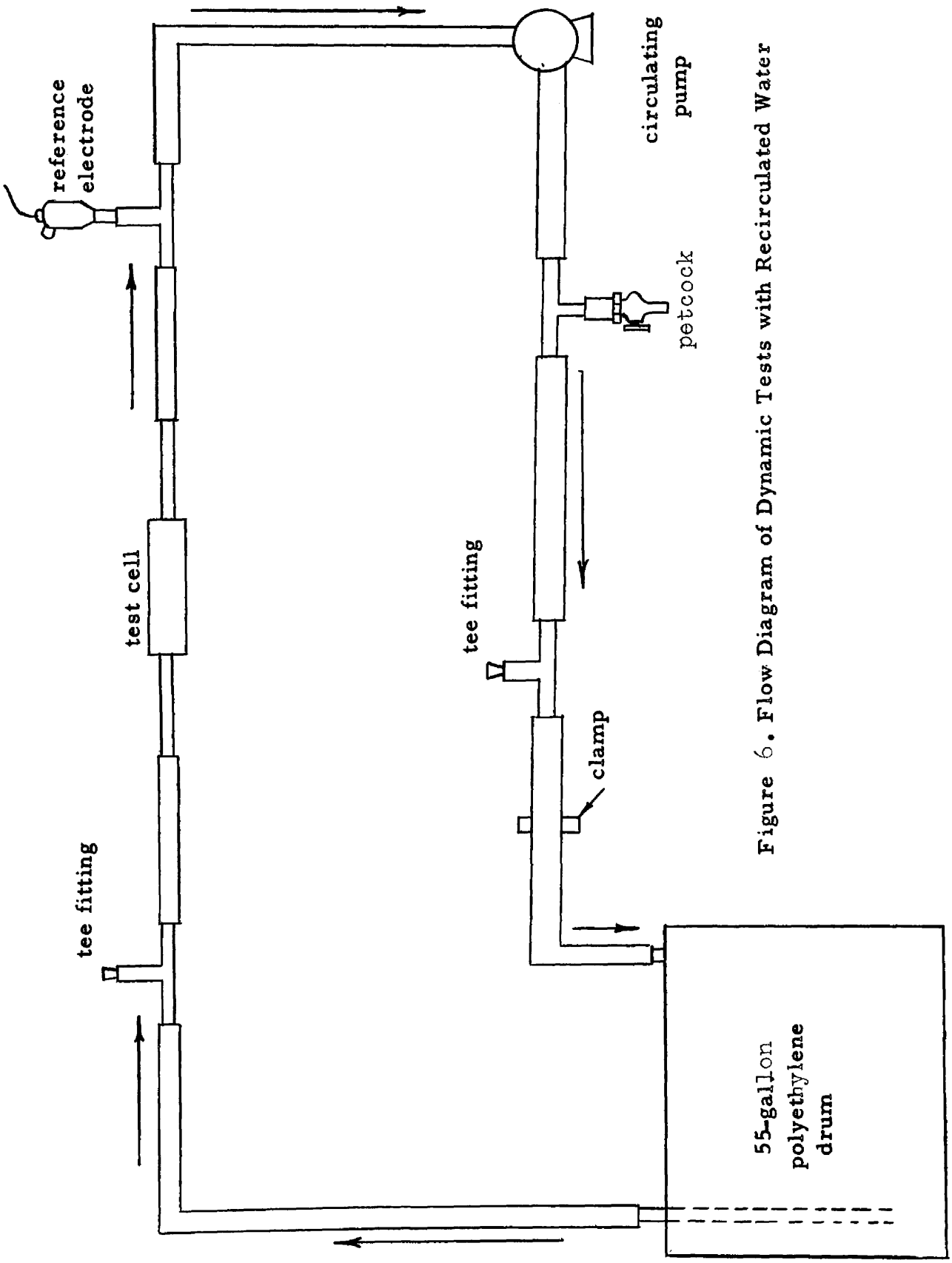

Figure 6. Flow Diagram of Dynamic Tests with Recirculated Water

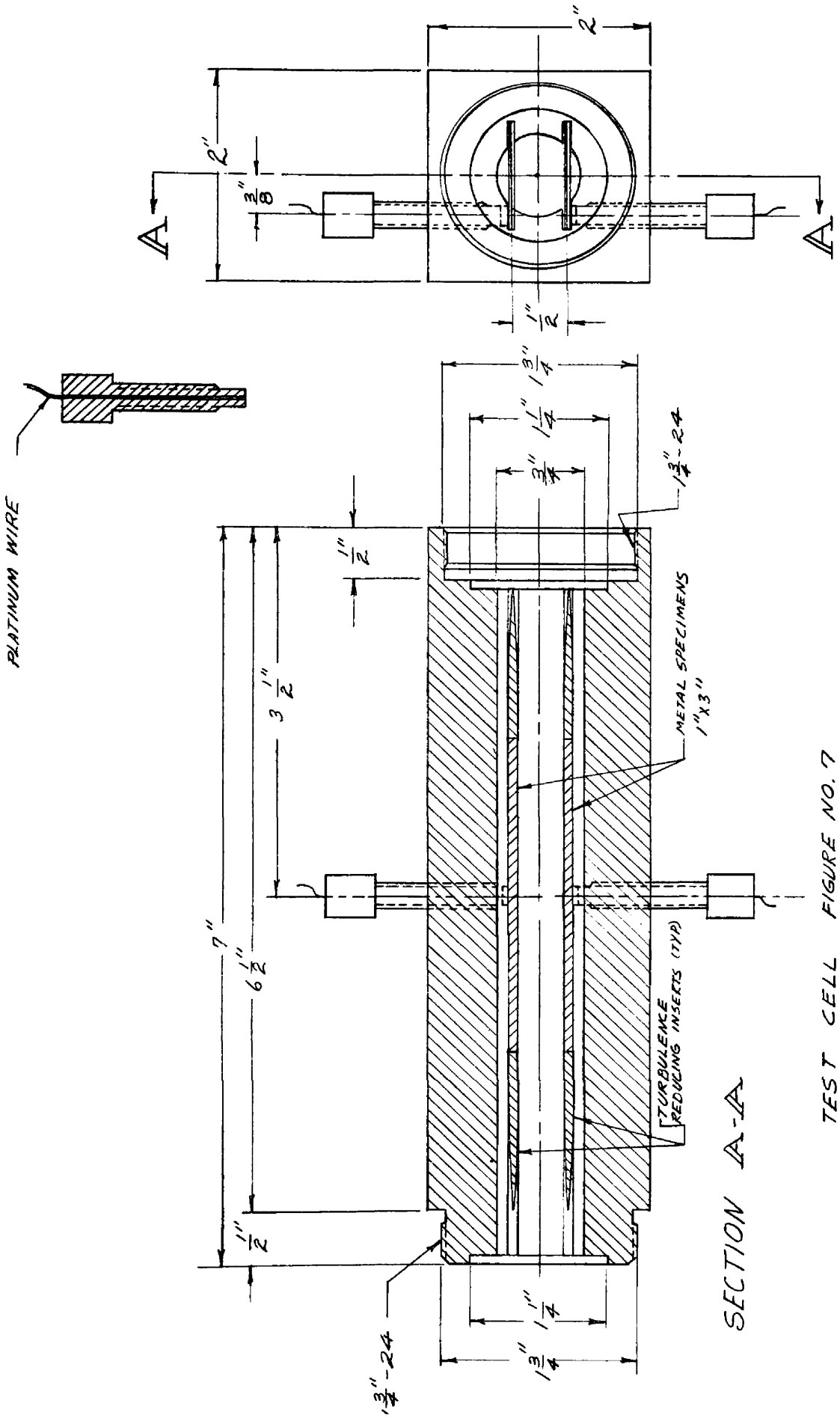

SECTION A-A

TEST CELL FIGURE NO. 7

the cell was drilled and tapped for potential measurements.

The cast iron or stainless steel specimens comprised the only metal in the system. All piping was Tygon tubing of 5/8-inch inside diameter and Van-Cor (unplasticized polyvinyl chloride) plastic fittings. The rate of flow was regulated by a clamp on the discharge side of the pump. As shown in the flow diagram of Figure 6, a saturated calomel electrode was inserted in the line through a tee fitting, to act as a reference electrode during potential measurements of the specimens. Saturated lime solution was added through the inlet tee fitting and carbon dioxide through the outlet fitting of the drum to adjust the water of the reservoir to the desired level of pH and hardness. Samples of the water were taken through a petcock fitting.

C. De-ionizing Units

All waters used for either static or dynamic tests were first passed through two de-ionizing units. The first unit was a large two-bed Lu-Hb Illco-Way deionizer shown in Figure 8. This unit was a strong-base ion-exchanger which could remove all ionizable solids including silica and CO_2. The water was then passed through a small mixed bed of Illco-Way research model de-ionizer. This small unit was also a strong-base ion-exchanger and could produce water

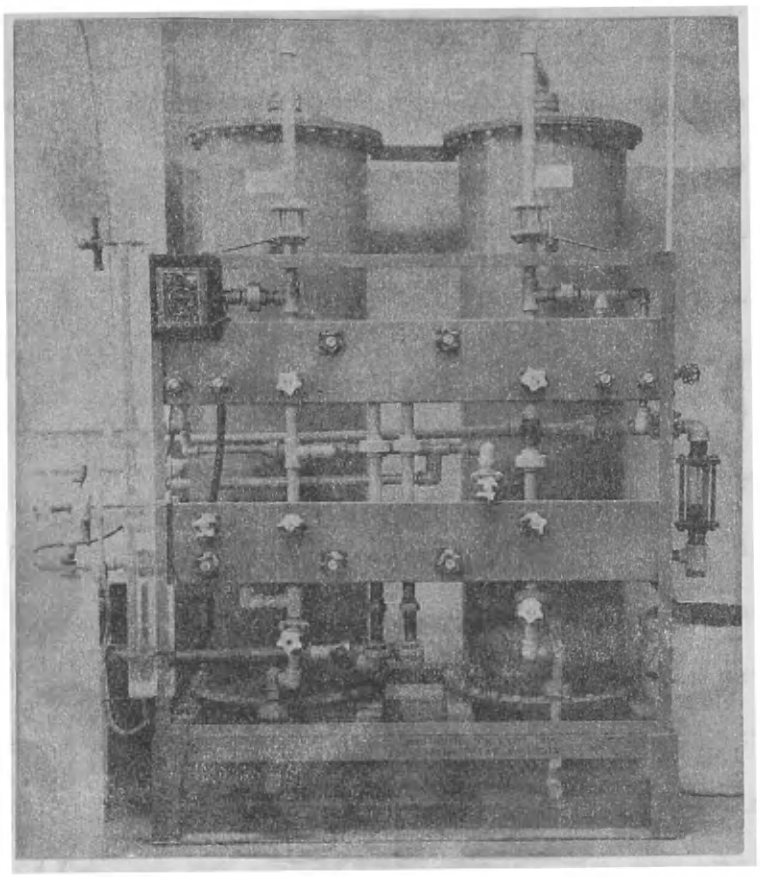

Figure 8.
The Large Two-Bed Ion-Exchanger

comparable to that produced by triple distillation.

D. Electrical Measurement Unit

1. Potentiometer

A Type K Leeds and Northrup Co. potentiometer was used during dynamic tests to measure the potential of the specimens with reference to a standard saturated calomel electrode. Figure 9 shows the potentiometer circuit and the electrical connections. The instrument consists of 15 five-ohm coils AD (adjusted to a high degree of accuracy) connected in series with an extended wire DB, the resistance of which is also five-ohms. A point M is arranged so that it can make contact between any two of the five-ohm coils and point M' is also arranged to make contact at any position on the extended wire DB. Current from batteries flows through these resistances and by means of regulating rheostat R is adjusted to one-fiftieth of an ampere. The potential drop across any one of the coils AD is consequently one-tenth of a volt and across the extended wire DB is 0.11 volt. By placing the contact point M' at zero and moving the contact M, the fall of potential between M and M' may be varied by steps of one-tenth volt, from 0 to 1.5 volts. The wire DB is divided into 1100 equal parts. By moving the contact point M' along the wire, the fall of

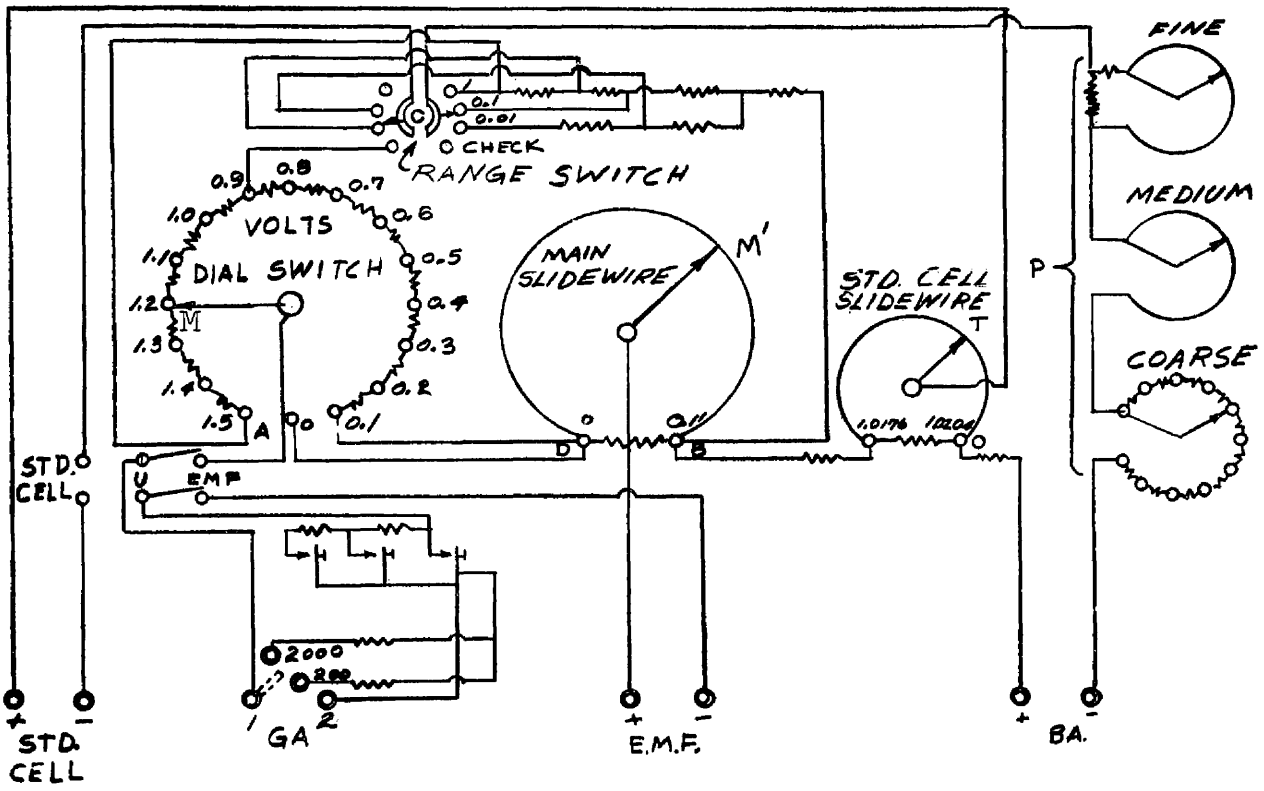

Figure 9. Potentiometer Circuit

potential between M and M' may be varied in infinitesimal steps.

To use this variable fall of potential in making measurements, convenient electromotive force is introduced in series with the galvanometer between the points M and M' and in opposition to the fall of potential along AB. The contact points M and M' are then adjusted until the galvanometer shows that no current is flowing, and the value of the electromotive force can then be read from the position M and M'.

2. Batteries

Two ignition dry cells, no. 6 IGN. 1 1/2 volts, Rayco type batteries were used in series to furnish a current which would produce a measurable fall of potential in the main circuit of the potentiometer.

3. Standard Cell

An Eppley standard cell of Eppley Laboratory, Inc., was used to regulate the current flowing through the wire AB of the potentiometer (Figure 9) and to make it exactly one-fiftieth of an ampere. The electromotive force of this cell is 1.01924 volts at 23° C. and has a temperature coefficient which is negligible within the ordinary range of room temperatures.

4. Galvanometer

The galvanometer used was a No. 2420 Leeds and Northrup Portable Lamp and Scale instrument. The galvanometer's function was to indicate the absence of current flow when connected in series with the unknown electromotive force between the regulated contact points M and M' of Figure 9. This galvanometer has a resistance of 1000 ohms; a period of 3 seconds; a sensitivity of 50 megohms; and is critically damped on open circuit.

5. DC Power Supply

A Model 600 B Sorensen and Company, Inc., DC variable voltage power supply was used to impress direct current through the specimens in some of the static and dynamic tests. The supply was also used to apply EMF across two platinum electrodes of the electrophoresis U-tube apparatus to determine the sign of electrical charge of colloidal particles. This instrument can be adjusted easily to any output voltage from 0 to 600 volts and is of negligible ripple.

EXPERIMENTAL PROCEDURE

A. Static Tests

De-ionized water used in all tests was first passed through the two-bed ion-exchanger in which the conductivity indicator indicated total solid content of the treated water to be less than one ppm equivalent of NaOH, and then through the small mixed-bed ion-exchanger. Saturated lime solution of certified Fisher reagent $Ca(OH)_2$, and carbon dioxide were added to the de-ionized water to produce water of the desired levels of pH and hardness.

Specimens were either cast iron or stainless steel. Cast iron specimens were 3.0 x 1.0 x 0.090 inch wafers sliced from cast iron bars and finished by surface grinding with a 40-grit diamond dressed wheel. Stainless steel specimens were 3.0 x 1.0 x 0.019 inch. The specimens were cleaned for five minutes in 0.1N HCl, washed with boiled de-ionized water, rinsed with acetone, dried and weighed before each test.

Specimens were totally immersed in make-up water of the desired pH and hardness, as described in the section on apparatus for static tests. The water was kept saturated

with oxygen and stirred throughout each run by bubbling air continuously and by keeping the cylinders open to the atmosphere.

In some tests a direct current was impressed through the specimens from the dc power supply by connecting the negative pole of the power supply to one specimen, which acted as a cathode, and the positive pole to other specimen, which acted as an anode. A 100,000-ohm variable decade resistance and model 374 Simpson ammeter were hooked in series with the specimens.

The duration of each run was exactly one week. Hardness and pH were adjusted to the desired level periodically throughout each run. All tests were conducted at room temperature.

B. Dynamic Tests with Recirculated Water

The circulating water was produced in the same manner as for the static tests, by adding saturated lime solution and carbon dioxide to demineralized water. Water was circulated through the test cell in which the specimens were mounted as has been described under the apparatus for dynamic tests.

In most runs, oxygen content of the water was kept within one ppm of saturation at room temperature by using

30 gallons of water in a 55-gallon reservoir with air filling the space above the water. The reservoir was also opened to the atmosphere several times during each run.

Some runs were conducted with water of different levels of dissolved oxygen. Some of these runs were made at a dissolved oxygen content below that of saturation while others were at levels higher than saturation. In low oxygen level studies forty gallons of water was held in the 55 gallons reservoir. Nitrogen was bubbled through this water at the beginning of the test for a period long enough to reduce the oxygen to the desired level. Different parts of the system were then connected so that the system was air tight. Care was taken to prevent any leakage of gases into or out of the system during the addition of lime solution and carbon dioxide. In this way it was possible to keep the oxygen content of the make-up water within one ppm of the desired level below saturation.

By following the same procedure as above and substituting oxygen for nitrogen, the dissolved oxygen content of the make-up water was maintained within one ppm of a desired level higher than that of saturation.

The pH and hardness of the water were adjusted periodically during each test. Specimens were cleaned and weighed before each test in the same manner as for the static tests. All runs were conducted at room temperature,

and at a linear velocity of 2 feet per second.

As in the static tests, in some runs a dc potential was impressed on the specimens, which acted as electrodes. The 100,000-ohm variable decade resistance and model 374 Simpson ammeter were connected with the specimen as shown in Figure 10. Polarization characteristics of the electrodes were measured at given intervals during a run by observing the potentials of each electrode against that of saturated calomel electrode at different applied current densities. The applied current density was kept constant throughout each run except when polarization measurements were made. During polarizing measurements different values of current densities were applied for few moments only.

In the majority of dynamic tests no outside current was impressed through the specimens. Corrosion potential of each specimen was measured at several intervals during a test by comparing the potential of the specimen with that of the reference saturated calomel electrode. Change of potential values of the specimen with time was a function of the action of the inhibitor on the corrosion tendency of the specimen. The potential of the specimen at the beginning of the test or at zero time was determined by immersing a similar specimen, cleaned in the same manner, in a beaker containing the same water as that of the test. The potential of the specimen was then quickly measured. With

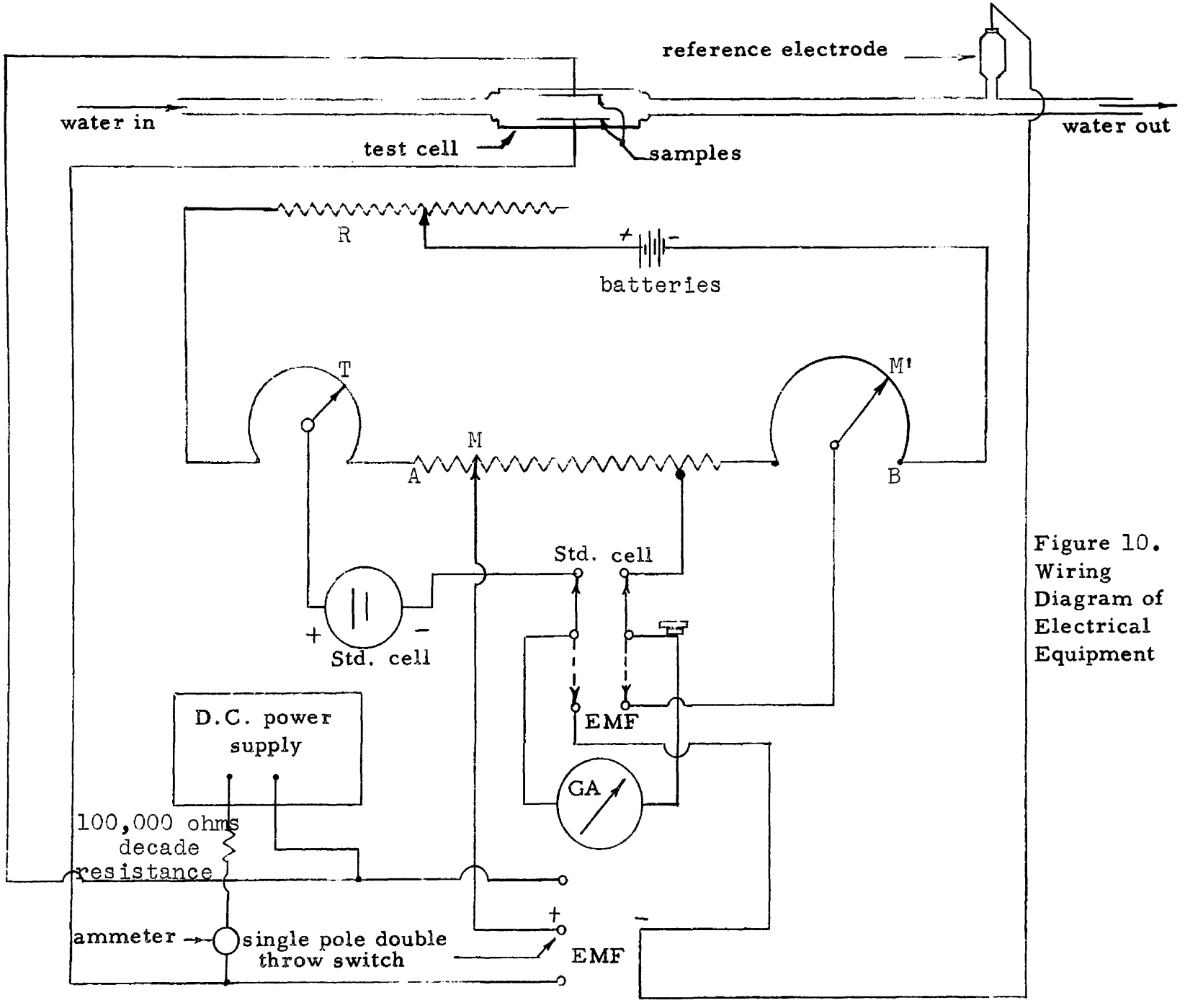

Figure 10. Wiring Diagram of Electrical Equipment

this method, the potential of the specimen at zero time could be determined more accurately than when the specimen was inside the test cell. It required only a few minutes for the recirculated water to fill all lines of the system at the beginning of each test. The change of potential of the specimen during this time was very sharp.

C. Specific Investigations

1. Potential Measurements

Potential measurements were made using a potentiometer and standard cell technique. The wiring diagram for these studies is shown in Figures 4, 9, and 10. The standard cell, galvanometer, and two batteries in series were connected to the main circuit of the potentiometer as shown in Figures 9 and 10. The current flowing in the wire AB was adjusted to one-fiftieth of an ampere by setting point T to correspond with the electromotive force of the standard cell (1.01924). The resistance R was regulated until the galvanometer showed no deflection.

The electromotive force of the electrochemical cell, in which the two electrodes were the specimen in the test cell and the saturated calomel electrode in the line, then replaced the electromotive force of the standard cell in the potentiometer circuit. The contact points M and M'

were manipulated until the galvanometer showed no deflection. The current was checked again by switching back to the electromotive force of the standard cell. If the galvanometer showed no deflection no further readjustment was needed. If a slight deflection occurred, a small readjustment of R and corresponding readjustment of M', after replacement of the applied electromotive force by that of the standard cell again, was required.

The reading of contact points M and M' then gave the potential value of the electrochemical cell composed of the specimen and the calomel electrode. Since the reference saturated electrode was assigned an arbitrary value of zero the cell potential then was that of the specimen serving as the second electrode in the electrochemical cell.

2. Preparation of Colloidal Calcium Carbonate

Two procedures were followed for preparation of colloidal calcium carbonate:

a. A supersaturated solution of $CaCO_3$ was prepared by addition of saturated lime solution and carbon dioxide to de-ionized water. Excess lime solution was then added to raise the pH to a value higher than 10. At this high pH colloids were formed and were prevented from growing into crystalline size by quickly adding CO_2 to bring the pH to a lower

value. This procedure resulted in the formation of a $CaCO_3$ suspension with a mixture of colloidal material which stayed in suspension and of larger crystals which precipitated.

b. Saturated lime solution and carbon dioxide were added to the demineralized water until colloids were observed at the desired pH level. It was found that by using this method, much finer colloids were produced than with the previous method. In most of the tests conducted in which the water contained colloidal $CaCO_3$ this latter method was utilized.

3. Determination of Electrical Charge of Colloids

Electrophoresis methods were used to determine the electrical charge of colloidal $CaCO_3$. The solution containing colloidal $CaCO_3$ was placed in a U-tube under the influence of an EMF applied through two platinum electrodes, one in each leg of the tube. Migration of the colloids then indicated the charge on the colloids. This migration was observed by noting the turbidity in the two legs of the U-tube after a few minutes of applied EMF. In cases where the solution contained a very small amount of colloidal $CaCO_3$, the migration could be seen by observing the scattering effect of a light beam at each electrode.

4. Analysis of Specimen Coatings After the Tests

Mineral examination was performed by the Michigan State University Geology Department by petrographic methods. Index oils of 1.58 and 1.80 were used. The mineral below 1.58 was calcite (calcium carbonate), the material above 1.80 was limonite (hydrous ferric oxide, chiefly goethite), and the intermediate mineral was siderite (ferrous carbonate). The percentage of each mineral was estimated by the above methods and identification and percentage values were checked by use of dilute hydrochloric acid for effervescent comparison. The minerals were also studies under crossed polarizing prisms, and the properties observed corresponded to those described for these minerals in textbooks on petrographic mineralogy.

5. Routine Analytical Determinations

The pH was determined using a Beckman Model H_2 Glass Electrode pH Meter. Analyses for total hardness and calcium hardness were by the Versenate method described in HachVer Catalog (33) of Hach Chemical Company. UniVer-1 indicator powder was used for total hardness and CalVer-11 indicator powder for calcium hardness.

Alkalinity, total iron content, and dissolved oxygen were determined by procedures described in the 10th edition of Standard Methods for the Examination of Water, Sewage,

and Industrial wastes (34). Total iron was determined using the Phenanthroline method. The Alsterberg Modification of the Winkler method for dissolved oxygen was followed with the exception that a round-bottom 250-ml flask with rubber stopper was used to collect the sample instead of the regular B.O.D. bottle. The rubber stopper contained two holes through which small glass tubes were inserted. It was possible, by this arrangement, to fill the flask with nitrogen gas before it was used to collect in the sample for dissolved oxygen determination.

CONDITIONS OF THE TESTS AND ANALYSIS OF THE COATINGS DEVELOPED

Table 1 shows various conditions of static tests and provides data concerning examinations and petrographic analyses of the coatings developed. Dynamic tests are shown in the same manner in Table 2.

All tests (static and dynamic) were conducted at room temperature. Duration of all static tests was one week. Recirculation of the make-up water of all dynamic tests was at a linear velocity of 2 feet per second past the specimens. In both types of tests water containing colloidal $CaCO_3$, the hardness reported included that of $CaCO_3$ colloids.

In both tables, where the test numbers carry a star, $CaCO_3$ colloids were prepared following the second procedure discussed under experimental procedure for preparing colloidal $CaCO_3$. That is, lime solution and CO_2 were added to the demineralized water until colloids were observed at the desired pH level.

In Table 1, an analysis of the coating of only one specimen is shown for some tests although two specimens were used in all static studies. The coatings of the other corresponding specimens were removed for weight loss

determinations. The test cell which was designed for only one specimen was used in some dynamic tests where the analysis of the coatings of only one specimen is reported.

Langelier's chart (6) was used to determine "saturation indices" graphically. "Stability indices" were calculated on the basis of pH_s values obtained from Langelier's chart. Values of "saturation excess" were determined experimentally using the "marble" test. The equation developed by Dye (32) was used to calculate "momentary excess" levels.

Terms used to describe coatings are as follows:

Blotchy: Irregular spots of large concentrations.

Powdery: Fine, loose particle appearance.

Tarnished: Discolored dull appearance.

Sugary: Granular appearance resembling sugar.

Spotty: Irregular spots of small concentrations.

Sparse: A coating of negligible amount.

Platy: Tendency to break off into sheets.

Table 1
Static Tests

Conditions of the Tests								Analysis of the Coatings					
Specimens	pH	Total hardness ppm equiv. of $CaCO_3$	Current impressed ma/in²	Other specifications of make-up water	Saturation index	Stability index	Saturation excess	Momentary excess	% Calcite $CaCO_3$	% Siderite $FeCO_3$	% Limonite $FeO(OH)$	Grain size (mm)	Macro description	Micro description
Cast iron cathode Cast iron anode	9.3	12	3.068	2 gms of ground $CaCO_3$ powder only was added to form the make-up water.					5 10	10 10	85 88	1/90 to 1/14 1/180 to 1/90	Fine grains, heavy coating of rust, very soft. Fine grains, heavy coating of rust, very soft.	Fine grains, heavy coating easily rubs off, coating 1/8 mm. in thickness. Fine grains, aggregates distribution, uniform coating, 0.25 mm. in thickness.
Cast iron cathode Cast iron anode	8.6	92	1.034	In addition, 1 gm of ground $CaCO_3$ powder was added.	+ .65	7.3	14.5	2.7	10 15	20 20	70 80	1/180 to 1/90 1/90 + or -	Blotchy, fine grains, slightly harder than anode coating. Blotchy, fine grains.	Scrapes off in plates, fine grained aggregates, uneven coating. Fine grained aggregates, uneven coating, coating heavier in center of plate.
Cast iron cathode Cast iron anode		92	1.034		+ .65	7.3	14.5	2.7	15 5	20 20	65 75	1/90 + or - 1/90 + or -	Fine grains, powdery. Blotchy, fine grains.	Aggregates up to 1 mm. in size, fine coating between aggregates. Fine grained aggregate, uneven blotchy coating.
Cast iron cathode Cast iron anode	8.6	92	1.034	Contained colloidal $CaCO_3$.	+ .65	7.3	14.5	2.7	10 5	15 10	75 85	1/90 + or - 1/180 to 1/90	Blotchy, fine grains. Blotchy, fine grains.	Aggregates dark in center, light around periphery, calcite found predominately between blotches, thin coating. Aggregates dark in center, light around periphery, calcite found predominately between blotches.
Cast iron specimen 1	8	92			+ .65	7.3	14.5	2.7	10	15	75	1/180 to 1/90	Fine grains, uneven coating.	Aggregates separated by fine coating.
Cast iron specimen 1	8.6	92		Contained colloidal $CaCO_3$.	+ .65	7.3	14.5	2.7	10	15	75	1/180 + or -	Powdery.	Aggregates of fine grains.
Cast iron specimen 1 Cast iron specimen 2	8.6	92		Powdered $CaCO_3$ ground in a ball mill for 6 days was used to form the make-up water.	+ .65	7.3	14.5	2.7	10 10	10 15	80 75	1/90 + or - 1/90 + or -	Blotchy, fine grains. Blotchy, fine grains.	Calcite predominates between blotches, thin film of calcite over blotches, rubs off readily. Calcite formed throughout plate, coating soft, easily scraped off.
Cast iron specimen 1	8.6	50			+ .15	8.3		0.4	5	20	75	1/180 to 1/90	Fine grains, uneven coating, soft.	Fine grains, uneven coating, ridge type, few distinct crystals, mostly aggregates.

Table 1 (II)
Static Tests

Test No.	Specimen	Conditions of the Tests: pH	Total hardness ppm equiv. of $CaCO_3$	Current impressed ma/da^2	Other specifications of make-up water	Saturation index	Stability index	Saturation excess	Momentary excess	Analysis of the Coatings: % Calcite $CaCO_3$	% Siderite $FeCO_3$	% Limonite $FeO(OH)$	Grain size (mm)	Macro description	Micro description
9	Cast iron specimen 1	8.6	50	0	Contained colloidal $CaCO_3$.	+ .15	8.3		0.4	5	20	75	1/90 + or -	Blotchy, fine grains.	Fine grained aggregate, uneven blotchy coating.
10	Cast iron specimen 1	9.0	92			+1.05	6.9		11.1	20	25	55	1/90 to 1/25	Blotchy, fine grains.	Coating readily scrapes off, uneven coating, well formed calcite crystals scattered throughout.
	Cast iron specimen 2									15	25	60	1/90 to 1/25	Blotchy, fine grains.	Rust aggregates through specimen, well formed calcite crystals found close to plate between heavy concentrations of limonite.
11	Cast iron specimen 1	9.0	92		Contained colloidal $CaCO_3$.	+1.05	6.9		11.1		10	85	1/90 + or -	Blotchy, darker staining in center of blotches.	Calcite crystals formed between blotches of siderite and limonite.
12	Cast iron specimen 1	9.0	50			+ .56	7.7		2.9	10	15		1/90 + or -	Blotchy, fine grains, rubs off easily.	Fine grained blotches of siderite, limonite, and calcite, well formed calcite crystals between blotches.
13*	Cast iron specimen 1	10.25			Contained colloidal $CaCO_3$.	+2.20	5.75	66.5	46.5	1-5	1-5	95	1/90 + or -	Very uneven distribution, rubs off easily.	Large uneven blotches of limonite, very soft, readily crumbles off.
	Cast iron specimen 2									1-5	1-5	95	1/90 + or -	Very uneven distribution, soft.	Massive uneven concentrations of limonite, calcite found throughout next to plate.
14	Platinum cathode Platinum anode	8	92	1.034		+ .65	7.3	14.5	2.7	100	---	---	1/90 to 1/45	Fine grains, even coating.	Even distribution, voids 1 to 4 times size of crystals.
										100	---	---	1/90 + or -	Fine grains, uneven distribution located at end.	Crystals present at one end of plate, voids 1 to 7 times size of crystals.
15	Stainless steel cathode Stainless steel anode	9.3	13	2.068	2 gms of ground $CaCO_3$ powder only was added to form the make-up water.					---	---	---	-------	Tarnished.	Very fine film.
16	Stainless steel cathode	8.6	92	1.034	In addition, 1 gm of ground $CaCO_3$ powder was added.	+ .65	7.3	14.5	2.7	100	---	---	1/25 + or -	Fine grains, even distribution.	Fine crystals, concentration poor, voids 1 to 10 times size of crystals.

Table 1 (III)
Static Tests

Test No.	Electrodes	Conditions of the Tests: pH	Total hardness ppm equiv. of $CaCO_3$	Current impressed ma/dm²	Other specifications of make-up water	Saturation index	Stability index	Saturation excess	Momentary excess	Analysis of the Coatings: % Calcite $CaCO_3$	% Siderite $FeCO_3$	% Limonite $FeO(OH)$	Grain size (mm)	Macro description	Micro description
[illegible]	Stainless steel anode									100	---	---	Less than 1/180	Very fine film.	Very fine grains, presence of calcite indicated by violent reaction with acid.
	Stainless steel cathode			1.034		+ .65	7.3	14.5	2.7	100	---	---	1/90 to 1/45	Fine grains, even coating.	Fine grains, even coating, voids few, those present 1 to 2 times size of crystals.
	Stainless steel anode									100	---	---	Less than 1/180	Very fine grains.	Very fine grains, uneven distribution.
9	Stainless steel cathode	8.6	92	2.068		+ .65	7.3	14.5	2.7	100	---	---	1/90 to 1/45	Fine grains, uneven coating.	Very few crystals or aggregates, coating present only at the center and at ends of plate.
	Stainless steel anode									---	---	---	-------	Tarnished.	Very fine film, no reaction with HCl.
9	Stainless steel cathode	8.6	92	2.068	Contained colloidal $CaCO_3$.	+ .65	7.3	14.5	2.7	100	---	---	1/90 to 1/45	Fine grains, even coating.	Spotty crystal distribution, voids 1 to 5 times size of crystals.
	Stainless steel anode									---	---	---	-------	Tarnished.	Very fine film, no reaction with HCl.
20	Stainless steel cathode	8.6	92	0.517		+ .65	7.3	14.5	2.7	100	---	---	1/90	-------	Few crystals scattered widely on plate.
	Stainless steel anode									100	---	---	1/90 + or -	Tarnished.	One or two crystals per ½ inch square area.
21	Stainless steel cathode	8.6	92	0.517	Contained colloidal $CaCO_3$.	+ .65	7.3	14.5	2.7	100	---	---	1/90 to 1/30	Fine sugary coating.	Few calcite crystals and aggregates, concentration poor.
	Stainless steel anode									---	---	---	-------	Tarnished.	No reaction with HCl.

Table 1 (IV)
Static Tests

Test No.	Steel	pH	Total hardness ppm equiv. of $CaCO_3$	Current impressed ma/ft²	Other specifications of make-up water	Saturation index	Stability index	Saturation excess	Momentary excess	% Calcite $CaCO_3$	% Siderite $FeCO_3$	% Limonite $FeO(OH)$	Grain size (mm)	Macro description	Micro description
22*	Stainless steel cathode Stainless steel anode	9.1	100	1.034	Contained colloidal $CaCO_3$.	+1.25	6.6		10.2	100	---	---	1/90 to 1/45	Spotty coating.	Voids 1 to 5 times crystal size.
										100	---	---	1/90 + or -	Spotty coating.	Voids 1 to 5 times crystal size.
23*	Stainless steel cathode Stainless steel anode	8.8	240	1.034	Contained colloidal $CaCO_3$.	+1.70	5.4		14.8	100	---	---	1/90 + or -	Granular coating.	Amorphous calcite, 1/30 crystalline granular appearance, voids 1 to 4 times crystal size.
										1000	---	---	1/90 to 1/45	Sparse distribution.	Crystalline and amorphous calcite present.
24*	Stainless steel cathode Stainless steel anode	9.5	70	1.034	Contained colloidal $CaCO_3$.	+1.35	6.8		14.9	100	---	---	1/90 to 1/25	Sparse coating.	Coating uneven.
										100	---	---	1/90 + or -	Uneven coating.	Coating uneven.
25*	Stainless steel cathode Stainless steel anode	9.1	150	1.034	Contained colloidal $CaCO_3$.	+1.60	5.9		17.1	100	---	---	1/90 + or -	Fine grains, uneven distribution.	One side of plate was even grain size, the other side showed variation in size 1/90 to 1/180.
										100	---	---	1/90	Fine grains, uneven distribution.	Even size grains throughout, voids 1 to 10 times crystal size.
26*	Stainless steel cathode Stainless steel anode	9.5	100	1.034	Contained colloidal $CaCO_3$.	+1.65	6.2		22.1	100	---	---	1/90 and 1/180	Uneven distribution.	Even distribution, voids 0 to 10 times crystal size.
										100	---	---	1/90 + or -	Uneven distribution.	Uneven distribution, size even, voids 0 to 20 times crystal size.
27*	Stainless steel cathode	10.25	83	1.034	Contained colloidal $CaCO_3$.	+2.20	5.85	66.5	46.5	100	---	---	1/90 + or -	Even coating.	Voids 1 to 5 times size of crystals.

Table 1 (V)
Static Tests

	Specimens	pH	Total hardness ppm equiv. of $CaCO_3$	Current impressed ma/dm²	Other specifications of make-up water	Saturation index	Stability index	Saturation excess	Momentary excess	% Calcite $CaCO_3$	% Siderite $FeCO_3$	% Limonite $FeO(OH)$	Grain size (mm)	Macro description	Micro description
	Stainless steel anode									100	---	---	1/180 to 1/90	Sparse distribution.	Coating easily rubs off, voids 1 to 10 times crystal size.
	Stainless steel specimen 1 sand blast	8.8	220		Contained colloidal $CaCO_3$.	+1.60	5.60		13.4	100	---	---	1/90 + or -	Fine grains, uneven distribution.	Crystals and aggregates tend to build up on one another, plate is pitted, crystals located around it.
	Stainless steel specimen 2 sand blast									100	---	---	1/90 + or -	Fine grains, uneven distribution.	Coating good, few voids, crystals closely packed.
79*	Stainless steel specimen 1	9	90		Contained colloidal $CaCO_3$ and iron oxide.	+1.65	6.30		24.0	98-99	---	---	1/90 + or -	Fine grains, hard coating.	Calcite discoloration due to $FeO(OH)$ present 1 - 2%.
	Stainless steel specimen 2									98-99	---	---	1/90 + or -	Fine grains, hard coating.	Same as Specimen 1.

Conditions of the Tests | Analysis of the Coatings

Table 2
Dynamic Tests

Test No.	Specimens	Conditions of the Tests: pH	Total hardness ppm equiv. of $CaCO_3$	Current impressed ma/ft²	Duration of test (days)	Dissolved oxygen (ppm)	Other specifications of make-up water	Saturation index	Stability index	Saturation excess	Momentary excess	Analysis of the Coatings: % Calcite $CaCO_3$	% Siderite $FeCO_3$	% Limonite $FeO(OH)$	Grain size (mm)	Macro description	Micro description
1	Cast iron cathode Cast iron anode	8.6	92	.[illegible]	7	Saturation		+ .65	7.3	14.5	2.7	15	15	70	1/90 + or -	Fine grains, linear coating.	Linear arrangement, calcite was predominate on top of the coating.
												10	10	80	1/90 + or -	Fine grains, linear coating.	Irregular linear coating.
2	Cast iron cathode Cast iron anode	8.6	92	.652		Saturation		+ .65	7.3	14.5	2.7	35	25	40	1/90 + or -	Fine grains, linear coating.	Linear arrangement.
												20	15	65	1/90 + or -	Fine grains, linear coating.	Ridges of limonite and siderite, calcite in valleys, amorphous calcite prominent over coating.
3	Cast iron cathode Cast iron anode		92	3.304		Saturation		+ .65	7.3	14.5	2.7	40	20	40	1/90 + or -	Platy coating.	Peels off in plates or sheets.
												30	20	50	1/90 to 1/30	Fine grains, linear coating.	Linear arrangement, calcite predominant on top of coating.
	Cast iron specimen 1	8.6	92			Saturation		+ .65	7.3	14.5	2.7	20	15	65	1/90 + or -	Linear spotty coating.	Ridges of siderite and limonite, calcite present overall. Calcite readily scrapes off.
	Cast iron specimen 2											15	10	75	1/90 + or -	Linear spotty coating.	Similar to Specimen 1, scrapes off more easily.
	Cast iron specimen 1	8.6	92			Saturation	Contained colloidal $CaCO_3$.	+ .65	7.3	14.5	2.7	10	10	80	1/180 to 1/25	Hard linear coating.	Particles vary in size from microscopic to aggregates, limonite in linear arrangement to calcite.
	Cast iron specimen 2											20	10	70	1/90 + or -	Coarse hard coating, linear arrangement.	Linear arrangement, hard coating, glassy texture on Fe mineral.
	Cast iron specimen 1	8.6	92			Saturation	Contained colloidal $CaCO_3$ ground in ball mill for 6 days.	+ .65	7.3	14.5	2.7	20	10	70	1/180 + or -	Heavy coating, calcite rubs off easily.	Fine powdery calcite aggregates overlying plate, ridges of limonite and siderite.
7*	Cast iron specimen 1	10.25	83			Saturation	Contained colloidal $CaCO_3$.	+2.20	5.85	66.5	46.5		30	30	1/90 + or -	Linear arrangement, soft and loose.	Calcite concentration in linear arrangement, also siderite and limonite linear concentration.

Table 2 (II)
Dynamic Tests

Test No.	Specimens	Conditions of the Tests: pH	Total hardness ppm equiv. of $CaCO_3$	Current impressed ma/dm²	Duration of test (days)	Dissolved oxygen (ppm)	Other specifications of make-up water	Saturation index	Stability index	Saturation excess	Momentary excess	Analysis of the Coatings: % Calcite $CaCO_3$	% Siderite $FeCO_3$	% Limonite $FeO(OH)$	Grain size (mm)	Macro description	Micro description
7*	Cast iron specimen 2											45	25	30	1/90 + or -	Linear, calcite loose.	Fine grained aggregates, linear arrangement, as in Specimen 1.
8*	Cast iron specimen 1	10.25	65			Saturation	Contained colloidal $CaCO_3$.	+2.05	6.15	48.5	34.7	1-3		95	1/180 to 1/25	Irregular coating.	Linear arrangement, light calcite film between limonite concentrations.
9	Cast iron specimen 1	8.6	150			Saturation	Contained colloidal $CaCO_3$.	+1.10	6.4	30.0	5.4	20	15	65	1/90 + or -	Medium hard, linear coating.	Arrangement similar to specimens of Test 4.
	Cast iron specimen 2											35	20	45	1/90 + or -	Medium hard, linear coating.	Linear coating, bonding not as good as Specimen 1.
10	Cast iron specimen 1	8.7	120			Saturation	Contained colloidal $CaCO_3$.	+1.0	6.7	22.0	5.1	10	10	80	1/180 + or -	Medium hard, fine linear coating.	Fine linear coating, granular calcite overlying plate, ridges of limonite and siderite.
11*	Cast iron specimen 1	8.4	205			Saturation	Contained colloidal $CaCO_3$.	+1.15	6.1	44.0	5.0	30	10	60	1/80 + or -	Medium hard, fine coating.	Calcite overlies limonite and siderite, limonite found next to plate, fine granular coating.
	Cast iron specimen 2 sand blast											30	10	60	1/180 + or -	Medium hard, fine coating.	Coating similar to Specimen 1.
12*	Cast iron specimen 1	8.3	200			Saturation	Contained colloidal $CaCO_3$.	+1.05	6.2	44.0	4.0	25	10	65	1/180 + or -	Fine, hard coating.	Even coating, grained calcite coating overlying limonite and siderite.
	Stainless steel specimen 2 sand blast											--	--	--	-----	No coating visible.	
13*	Cast iron specimen 1	8.3	200			Saturation	Contained colloidal $CaCO_3$.	+1.05	6.2	44.0	4.0	30	10	60	1/180 + or -	Fine, hard, sugary coating.	Even coating tending for linear arrangement, calcite overlies siderite and limonite.
	Stainless steel specimen 2											--	--	--	-----	No significant deposit.	

Table 2 (III)
Dynamic Tests

Test No.	Specimens	Conditions of the Tests: pH	Total hardness ppm equiv. of $CaCO_3$	Current impressed ma/ft²	Duration of test (days)	Dissolved oxygen (ppm)	Other specifications of make-up water	Saturation index	Stability index	Saturation excess	Momentary excess	Analysis of the Coatings: % Calcite $CaCO_3$	% Siderite $FeCO_3$	% Limonite FeO(OH)	Grain size (mm)	Macro description	Micro description
14*	Cast iron specimen 1	8.3	200	0	1	Saturation	Contained colloidal $CaCO_3$.	+1.05	6.2	44.0	4.0	40	10	50	1/180 + or -	Fine grains, soft coating.	Soft coating.
15*	Cast iron specimen 1	8.3	200			Saturation	Contained colloidal $CaCO_3$.	+1.05	6.2	44	4.0	15	5	75	1/90 to 1/180	Hard coating, linear arrangement.	Contained 5% magnetite, limonite ranges in hardness from 2 to 5, blotches of hard limonite, calcite overlies soft limonite, magnetite and siderite dispersed throughout.
16*	Cast iron specimen 1	8.3	200			Saturation	Contained colloidal $CaCO_3$.	+1.05	6.2	44	4.0	10	10	80	1/90 to 1/180	Soft coating, linear arrangement.	Ridges of limonite flat and tend to break off into plates, calcite mainly in the valleys.
17*	Cast iron specimen 1	10.25	65			1.5 - 2.5	Contained colloidal $CaCO_3$.	+2.05	6.15	40.5	34.7	10	5	20	1/180 + or -	Uneven, medium hard coating.	Contained 65% magnetite, linear arrangement, calcite found in between ridges of magnetite and siderite.
18*	Cast iron specimen 1	8.3	200			1.7 - 2.7	Contained colloidal $CaCO_3$.	+1.05	6.2	44	4.0	30	20	50	1/180 to 1/90	Soft coating, linear arrangement.	Siderite and limonite predominate close to plate, amorphous calcite overlies coating and predominates in valleys.
19*	Cast iron specimen 1	8.3	200			27 - 28	Contained colloidal $CaCO_3$.	+1.05	6.2	44	4.0	20	15	63	1/90	Even, soft coating.	Contained 2% magnetite, limonite harder, siderite and magnetite coating to plate overlies by amorphous calcite.
	Cast iron specimen 2											20	15	63	1/90	Even, soft coating.	Contained 2% magnetite, similar to Specimen 1, however calcite more intermixed instead of predominating over coating.
20*	Cast iron specimen 1	8.3	180			0.88 - 2.1	Contained colloidal $CaCO_3$.	+ .95	6.4		3.2	10	10	80	1/180	Fine grains, soft coating.	Contained 1% magnetite, coating flaky tends to break off in sheets, very little calcite next to plate, limonite, siderite and magnetite predominate next to plate.

Table 2 (IV)
Dynamic Tests

Conditions of the Tests										Analysis of the Coatings					
Specimens	pH	Total hardness ppm equiv. of $CaCO_3$	Current impressed ma/dm^2	Duration of test (days)	Dissolved oxygen (ppm)	Other specifications of make-up water	Saturation index	Stability index	Saturation excess	Momentary excess	% Calcite $CaCO_3$	% Siderite $FeCO_3$	% Limonite $FeO(OH)$	Grain size (mm)	Macro description	Micro description
Cast iron specimen 1	8.3	180	0	3	4 - 5	Contained colloidal $CaCO_3$.	+ .95	6.4		3.2	25	15	60	1/180	Fine grains, soft coating.	Contained 1% magnetite, linear arrangement, calcite overlies ridges of limonite and siderite, calcite also found in valleys, intermixture of all present near plate.
Cast iron specimen 1	8.3	180			Saturation	Contained colloidal $CaCO_3$.	+ .95	6.4		3.2	25	20	55	1/180	Linear arrangement, medium hard coating.	Contained 1% magnetite, blotches in linear arrangement, amorphous calcite intermixed throughout.
Cast iron specimen 1	8.3	180			Saturation	Contained colloidal $CaCO_3$.	+ .95	6.4		3.2	25	20	55	1/180	Linear arrangement, medium hard coating.	Limonite predominates near plate, calcite overlies coating.
Cast iron specimen 2											25	20	55	1/180	Linear arrangement, medium hard coating.	Same as Specimen 1.
Cast iron specimen 1	8.3	180			10 - 11	Contained colloidal $CaCO_3$.	+ .95	6.4		3.2	10	10	78	1/90	Uneven, medium hard coating.	Contained 2% magnetite, irregular blotchy coating, blotches in linear arrangement, calcite overlies plate, limonite, siderite and magnetite next to plate.
Cast iron specimen 2											10	10	79	1/90 to 1/180	Uneven, medium hard coating.	Similar to Specimen 1.
Stainless steel specimen 1	8.3	200			Saturation	Contained colloidal $CaCO_3$ and iron oxide.	+1.05	6.2		44	98		1-2	1/180	Uneven, medium hard coating.	Amorphous calcite coating more prominent where limonite present, coating tends to be at one end of plate and opposite on the other side, voids 1 to 10 times size of particles.

DISCUSSION OF RESULTS

Mineral Content of Developed Coatings

Examination of minerals developed upon the cast iron specimens showed that coatings consisted of mixtures of limonite (hydrous ferric oxide, chiefly goethite), calcite (calcium carbonate) and siderite (ferrous carbonate). Magnetite was also present in some tests, usually covered by limonite. With stainless steel specimens only calcite was found.

Microscopic examination revealed a linear arrangement of ridges and valleys on cast iron specimens from the majority of tests. This linear arrangement was particularly noticeable for specimens from dynamic tests. Most of the calcite observed was found in the valleys, while ridges were commonly limonite on the surface with siderite near the metal.

Calcite showed typical rhombohedrals on the stainless steel specimens. In the valleys of cast iron specimens some calcium carbonate crystals were noted but the calcite was commonly amorphous. Ridges were predominantly hydrous ferric oxide in the form of limonite with some calcite often present on the top. Siderite was commonly found in

very fine crystals. Limonite was not crystalline, being observed in the amorphous form only.

Percentages of the siderite constituent of coatings very closely followed that of calcite. Magnetite was found in amorphous form only.

Polarization Studies

The significance of polarization studies in investigating the action of a corrosion inhibitor has been discussed previously under theoretical considerations. These studies were undertaken for the purpose of determining the function of calcium carbonate as a corrosion inhibitor.

In the first three dynamic runs, studies were made using a galvanic couple of cast iron specimens mounted in the test cell of the flow system. These runs were conducted at a pH level of 8.6, a hardness of 86 ppm equivalent of $CaCO_3$, water saturated with dissolved oxygen, and no colloidal $CaCO_3$ present. The applied current density was the only variable in the testing conditions of the runs.

Direct current was applied through the specimens, which acted as electrodes, from the dc power supply. Current densities of 0.826, 1.652, and 3.304 ma/dm^2 were respectively applied in these three runs. Polarization characteristics of the electrodes were determined according

to the method discussed under experimental procedure.

Figures 11, 12, and 13 show polarization characteristics of the anodes and cathodes for the three tests. In each case the upper curves represent the potential values of the cathode at the indicated rate of applied current density between the electrodes. The lower curves show the potential-current density characteristics of the anode. Percent compositions of the coatings developed after 7 days period are shown in Table 3.

Figure 11 shows polarization curves which were obtained at the applied current density of 0.826 ma/dm^2. These curves show that the corrosion was essentially under mixed control for the entire test.

At applied current densities of 1.652 and 3.304 ma/dm^2 Table 3 indicates that more calcium carbonate was deposited on both cathodes and anodes. Polarization curves obtained at these higher current densities are shown in Figures 12 and 13. Comparison of the curves in Figures 12 and 13 with those in Figure 11 reveals that the only noticeable change which took place as result of deposition of more $CaCO_3$ was increased polarization of the cathodes as the tests progressed. This increased cathode polarization, as measured by the slopes of the cathode curves, was more pronounced in Figure 13 where more $CaCO_3$ was deposited on the electrodes. Open-circuit potentials of the cathode curves of Figures 12

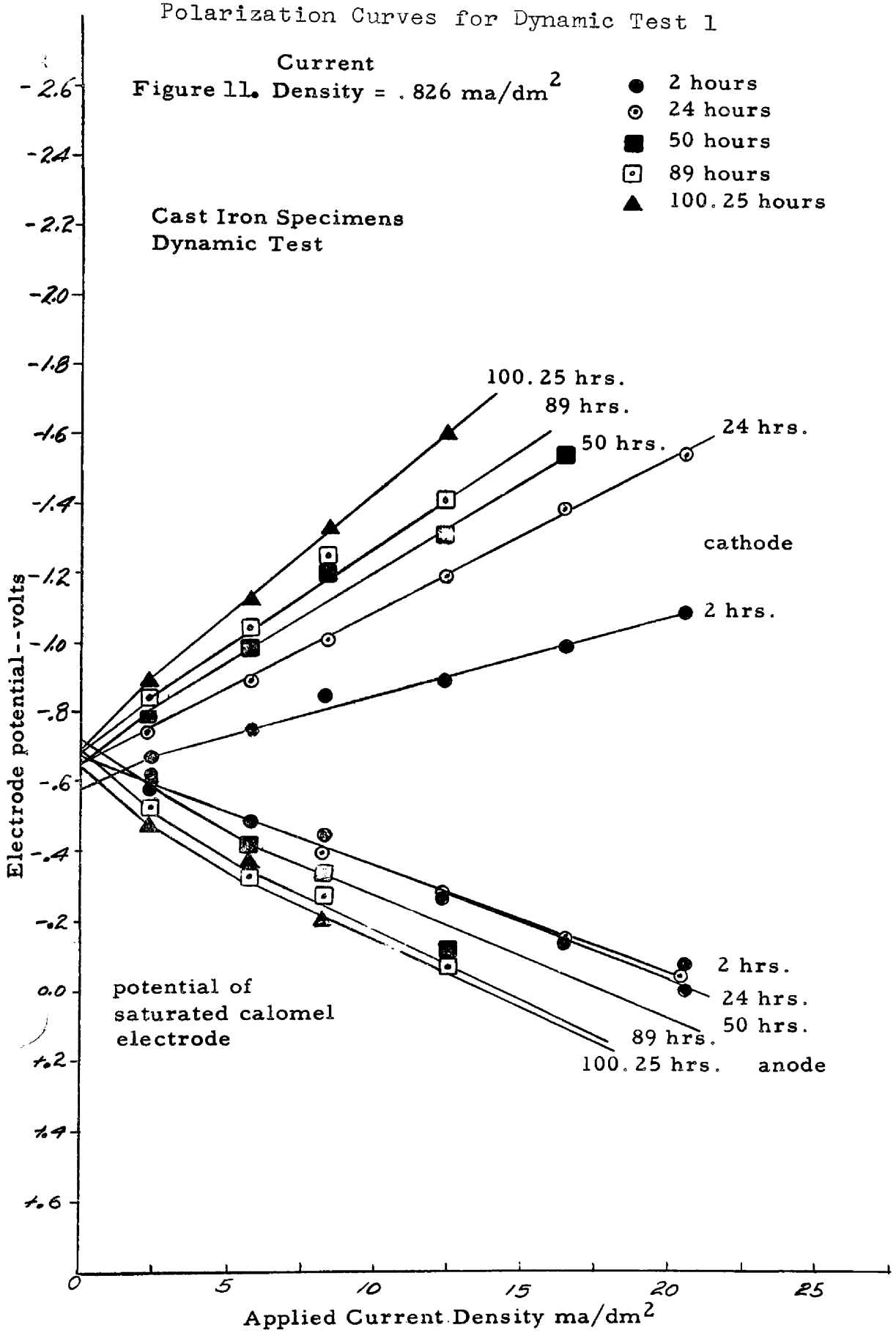
Polarization Curves for Dynamic Test 1
Current
Figure 11. Density = .826 ma/dm2
2 hours
24 hours
50 hours
89 hours
100.25 hours
Cast Iron Specimens
Dynamic Test
100.25 hrs.
89 hrs.
50 hrs.
24 hrs.
cathode
2 hrs.
2 hrs.
24 hrs.
50 hrs.
89 hrs.
100.25 hrs.
anode
potential of
saturated calomel
electrode
Electrode potential--volts
-2.6
-2.4
-2.2
-2.0
-1.8
-1.6
-1.4
-1.2
-1.0
-.8
-.6
-.4
-.2
0.0
+.2
+.4
+.6
0
5
10
15
20
25
Applied Current Density ma/dm2

Polarization Curves for Dynamic Test 2

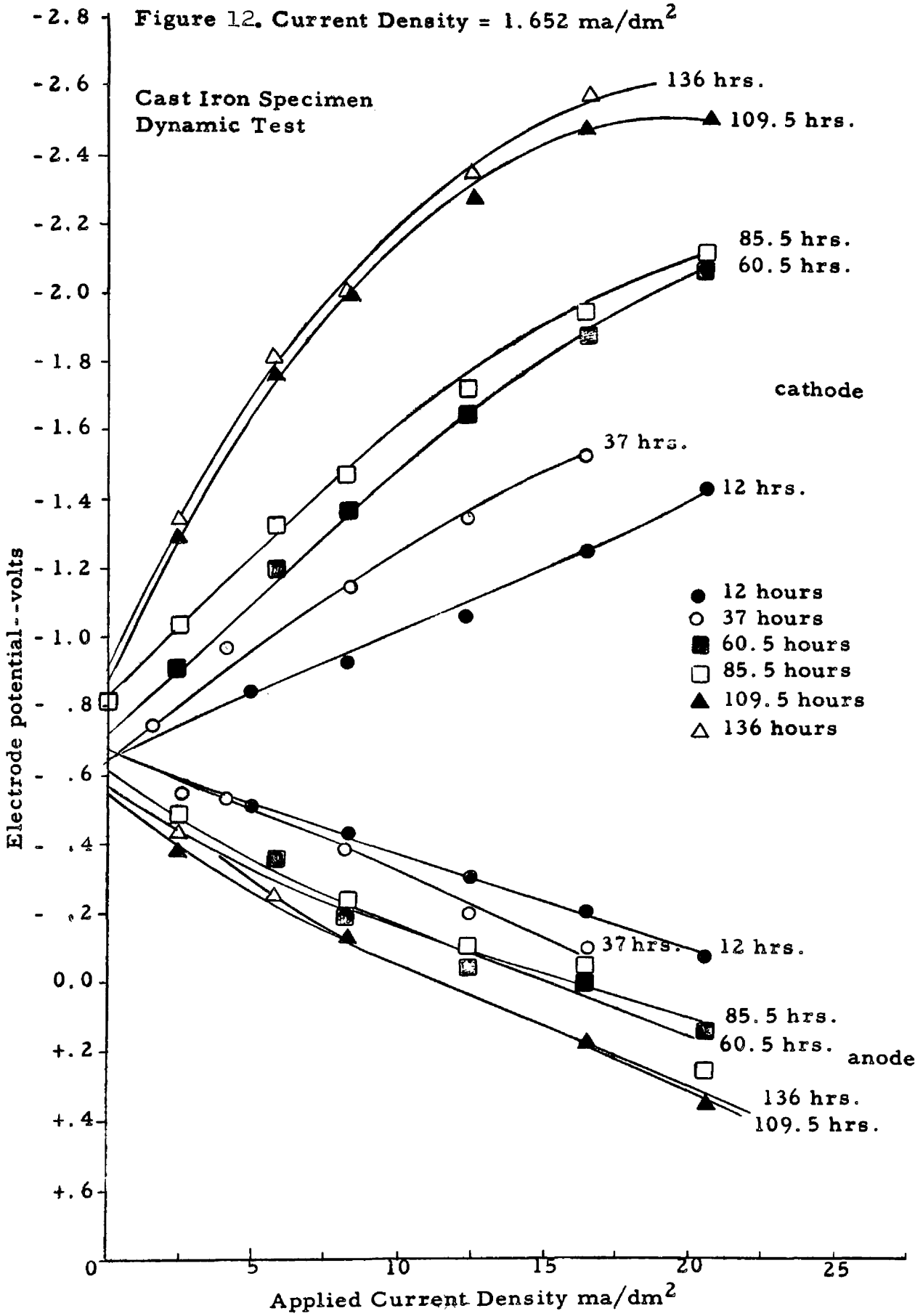

Polarization Curves for Dynamic Test 3

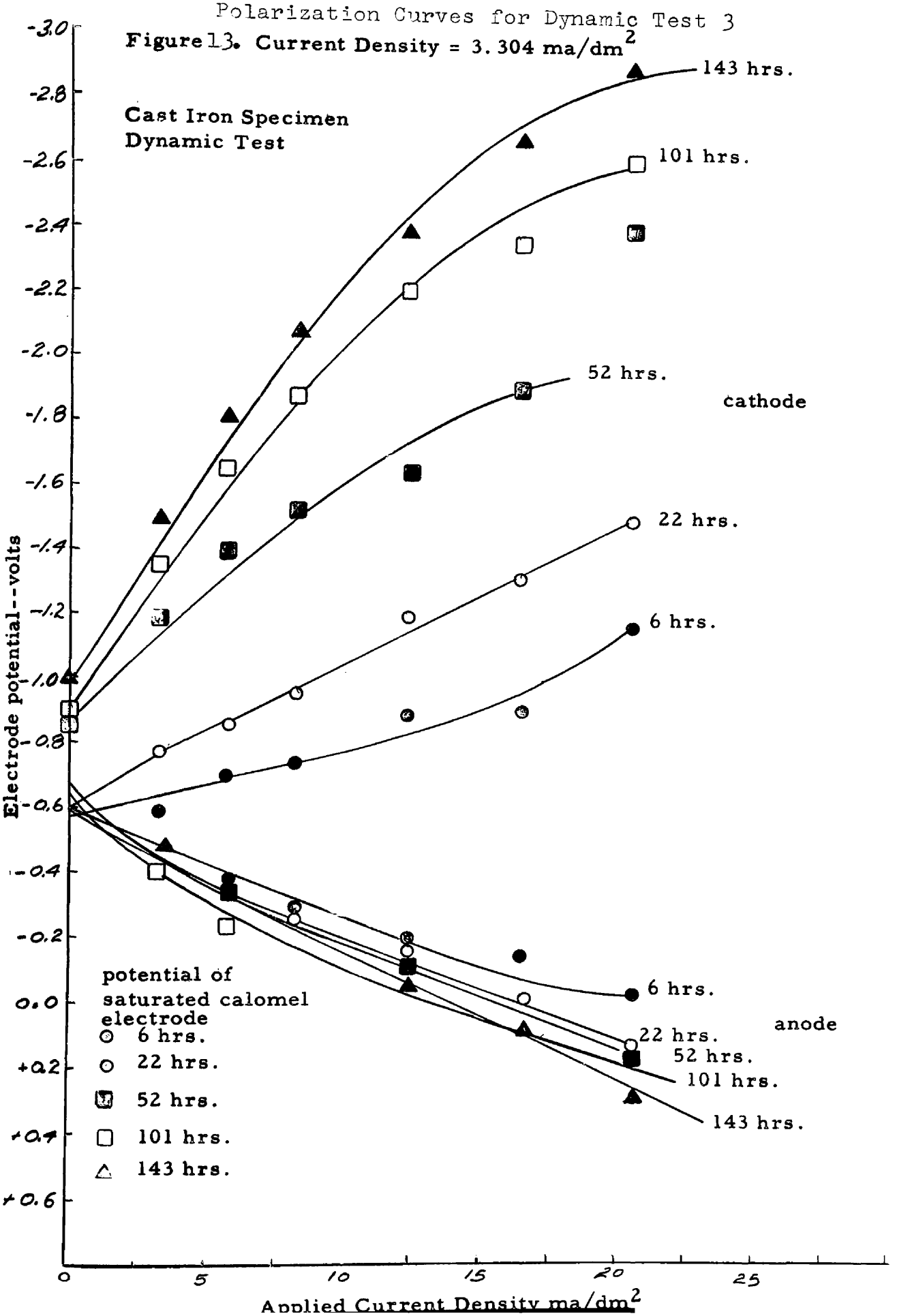

Table 3
% Composition of Specimen Coatings for
the First Three Dynamic Tests

Test no.	Applied current density ma/dm^2	Electrode	% $CaCO_3$	% $FeCO_3$	% FeO(OH)
	0.826	Cathode	15	15	70
		Anode	10	10	80
2	1.652	Cathode	35	25	40
		Anode	20	15	65
3	3.304	Cathode	40	20	40
		Anode	30	20	50

and 13 also show a significant shift in the cathodic or more noble direction as the tests progressed.

Anode polarization curves of Figures 12 and 13 show no significant change in polarization or open circuit potentials as compared with those of Figure 11 although more $CaCO_3$ has been deposited on the anodes. This indicated that calcium carbonate had no inhibitory action on the anodes of the galvanic couples.

From the above discussion, it may be stated that calcium carbonate acted primarily as a cathodic inhibitor on cast iron specimens.

Table 3 indicates more $CaCO_3$ deposited on cathode than on anode specimens. The neutralization of hydrogen ions in the solution at the cathode resulted in the production of alkaline condition in the vicinity of this electrode, as has been discussed under theoretical considerations. An increase in the pH value of the solution near the cathode would then be produced which shifted the $CaCO_3$ equilibrium in such a way to favor more deposition in that region.

Formation of Colloidal $CaCO_3$

It is to be recalled that two procedures were followed for preparation of colloidal $CaCO_3$ by the addition of lime solution and carbon dioxide to demineralized water. In the

first method, the pH was allowed to rise to a value higher than 10 by adding excess lime water to a supersaturated solution of $CaCO_3$. Colloids formed were prevented from growing into crystalline size by quickly adding CO_2 to bring the pH to a lower desired level. In the second and most used method, the pH was held at a predetermined level while lime solution and carbon dioxide were added to de-ionized water until colloidal $CaCO_3$ appeared.

An investigation was made of the degree of supersaturation of $CaCO_3$ solution at which colloidal particles were formed at different levels of pH. Carbon dioxide and saturated lime solution were added simultaneously to two liters of de-ionized water in a 4-liter flask. The addition of these two chemicals, after saturation conditions had been reached, was carefully regulated so that the pH level of the solution was maintained at a desired level. Ten minutes after each 2-ml addition of saturated lime water and corresponding addition of CO_2, the solution was examined for colloidal particles of $CaCO_3$. The scattering effect of a light beam was used as an indication of the presence of colloids. A slight drop in pH value was another indication of colloid formation.

Table 4 shows pH and hardness values corresponding to the supersaturation levels at which colloidal $CaCO_3$ appeared. Values of "momentary excess" and "saturation

Table 4
Formation of Colloidal $CaCO_3$ Particles

pH	Hardness ppm equivalent of $CaCO_3$	Saturation excess	Momentary excess
8.8	271	99	17.4
9.2	211	91	29.8
9.6	96	53	25.9
10.25	83	66.5	46.5

excess" corresponding to these levels of supersaturation are also shown.

Values of pH were plotted against values of "momentary excess" and "saturation excess" as shown in Figure 14. This figure indicates the "momentary excess" and "saturation excess" values for supersaturated solutions at which $CaCO_3$ colloids formed at different pH levels. Values of "momentary excess" required to precipitate colloidal particles out of solution were higher as the pH levels increased. Values of "saturation excess," however, decreased as pH levels acquired higher values.

Condensation of molecules and ions into colloidal particles has been examined comprehensively by von Weimarn (35). He concluded that relative supersaturation, not absolute supersaturation, governed the rate of nucleus formation of these particles. The ratio of "momentary excess" of supersaturated solution to the solubility of $CaCO_3$ in solution can be defined, in this case, as the relative supersaturation. The solubility of $CaCO_3$ in water is constant at all pH levels. Formation of colloidal $CaCO_3$, thus, should not be influenced by the pH level of the solution and should be a function of "momentary excess" values of solution only.

Variation of "momentary excess" values with pH levels may be due to the temporary production of local areas of

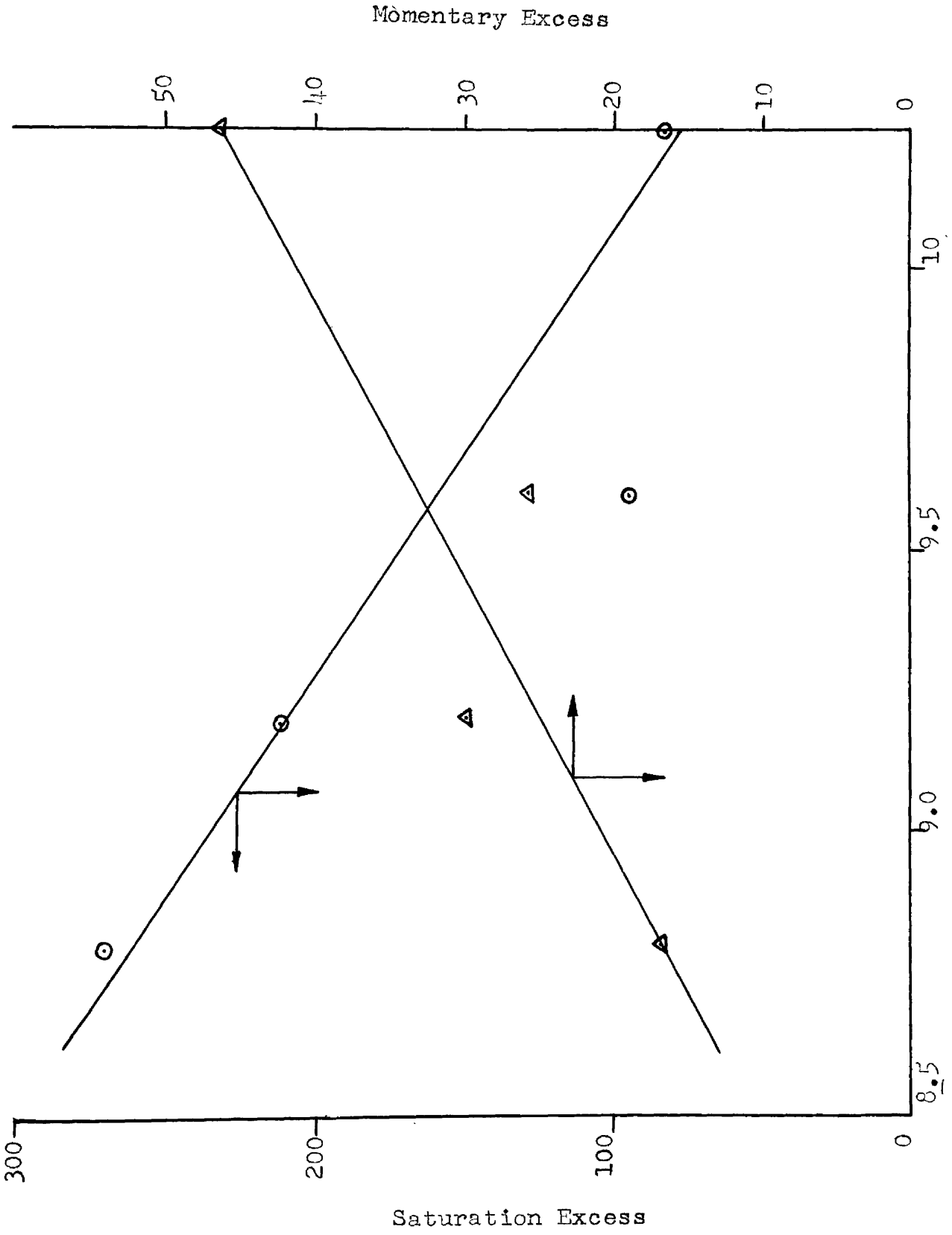

Figure 14 - Formation of Colloidal $CaCO_3$

very high supersaturation. Two supersaturated solutions of the same "momentary excess" values but at different pH levels contain different concentrations of calcium, carbonate, bicarbonate, and hydroxide ions. The solution of the lower pH level contains relatively higher concentrations of calcium and bicarbonate ions and relatively lower concentrations of carbonate and hydroxide ions. By adding 2 ml of lime water to low pH solutions, a higher temporary "momentary excess" value is created locally in the areas where lime water is only partly mixed with the main body of the solutions, and bicarbonate ions are converted into carbonate ions. In addition, a heavy concentration of calcium ions also exists in local areas of this solution. Colloids may thus be formed locally in these overconcentrated areas. Redissolving of colloidal particles once formed is a very slow process. The colloids formed may also act as nuclei to further aid $CaCO_3$ precipitation.

There is less chance of forming these temporary local areas of very high supersaturation by addition of 2 ml of lime water to high pH solution. There are relatively few bicarbonate ions to be converted into carbonate ions and the concentration of calcium ions is relatively low too.

Calcium carbonate colloids were also prepared by grinding $CaCO_3$ powder in a ball mill for 6 days. Some $CaCO_3$ colloids were formed when this powder was added to de-ionized

water. Colloids prepared in this manner were used in Dynamic Test 7 and Static Test 20. It was found that these colloids were very unstable, precipitated heavily, and did not produce favorable coatings.

Electrical Charge of Colloidal $CaCO_3$

It was found that colloidal calcium carbonate particles, in the pH range of 6 - 11, always migrated to the cathode when placed in an electric field of an electrophoresis apparatus. This observation indicated that these colloidal particles carried positive charges. Such finding was not in agreement with that of Larson and Buswell (36) who have stated that calcium carbonate had a negative charge in the presence of calcium bicarbonate as well as in the presence of calcium hydroxide.

In order to check further, the following tests were made:

1. De-ionized water was distilled twice and used to dissolve Fisher certified reagent $Ca(OH)_2$ to form colloidal $CaCO_3$. The resulting colloids showed a positive charge in the pH range of 6 - 11.
2. Colloidal $CaCO_3$ was prepared from lime water, and excess Na_2CO_3 and CO_2 added. The colloid formed showed a positive charge.

3. Moderate concentrations of $CaCl_2$ and Na_2CO_3 were mixed to prepare colloidal $CaCO_3$, which showed a positive charge.
4. $CaCO_3$ powder was ground in a ball mill for 6 days. Some $CaCO_3$ colloids were formed when this ground powder was added to de-ionized water. The colloids once again showed a positive charge.
5. A current was impressed through two stainless steel specimens, one acting as the cathode and the other as the anode. The solution contained colloidal $CaCO_3$. More $CaCO_3$ was deposited upon the cathode than the anode.

Upon the basis of these experiments, it was concluded that colloidal $CaCO_3$ has a positive charge in the pH range 6 - 11.

The electrical charge carried by colloidal particles is of fundamental importance, because without this charge colloidal systems are unstable. The source of the charge is explained by the so-called electrical double layer theory. This theory assumes that a layer consisting of two parts surrounds the colloidal particle. The first layer approximately a single ion in thickness, remains firmly attached to the wall or surface of the solid phase and determines the charge. The second part of the double layer extends some distance into the liquid phase and is considered movable.

Since a colloidal $CaCO_3$ particle travels to the cathode when placed in an electric field it may be assumed that such a particle has preferentially adsorbed calcium ions from the solution, thus localizing a number of positive charges in the immediate neighborhood of the particle's surface. The hydroxyl ions may be assumed as the second part of the double layer which is associated with adsorbed calcium ions and is dispersed around the particle at a certain average distance from it as shown in Figure 15. The concentration of hydroxyl ions is only slightly greater around the particle than in the main body of solution. Colloidal calcium carbonate particle may thus be represented by $(CaCO_3)Ca^{++}\vdots OH^-$ where $(CaCO_3)$ implies a particle of calcium carbonate and the dotted lime indicates approximately the limit of the fixed part of the double layer.

Effect of Colloidal $CaCO_3$ on Coatings Developed

Most static and dynamic tests were conducted with calcium carbonate present in colloidal form. Hard, dense, protective coatings, with good bonding to the metal surface, were generally obtained in the presence of the colloids. This was especially true for coatings on specimens obtained with dynamic tests. Coatings from tests made under identical conditions without colloidal material present were

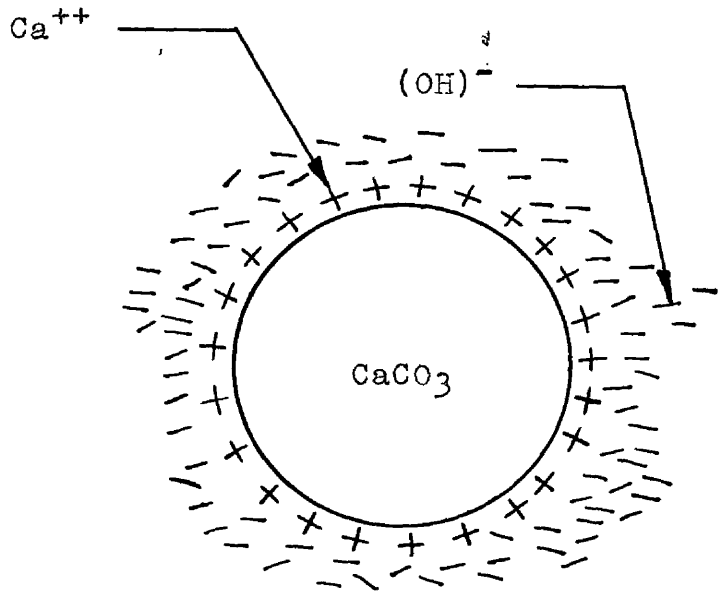

Figure 15 - Schematic Diagram of Colloidal $CaCO_3$ Particle

softer and formed a poorer bond to the metal.

Microscopic examination and petrographic analysis of the coatings revealed that the action of colloidal $CaCO_3$ was to improve the bonding and hardness of corrosion products, especially limonite. Limonite present in coatings obtained in presence of colloidal $CaCO_3$ was harder in Moh's hardness scale and darker in color as compared with that formed under similar conditions without colloids. Calcite and limonite were found in physical but not chemical mixture.

Coatings obtained from some specimens under dynamic tests in the presence of $CaCO_3$ colloids consisted of a uniform clinging protective mixture of limonite, siderite, and calcite. This material formed the entire coating including the innermost layer next to the surface of metal. This mixture bonded well to the cast iron specimens and was hard and relatively tough. Coatings obtained from tests where colloidal material was absent were quite different. In this case the layer at the metal surface was found to be formed of loose grains of limonite over which layers of mixed, unpacked grains of calcite, siderite and limonite we were built up.

In dynamic tests a greater tendency to form linear arrangements characterized coatings obtained in the presence of colloids as compared to those obtained under similar

conditions without colloids. In static tests, when colloids were present the coatings consisted of calcite distributed between blotches of limonite and siderite. In the absence of colloids, under identical static test conditions, coatings were composed of loose grained mixtures of calcite, limonite and siderite. Generally, the size of grains forming the coatings was slightly greater where colloids were present.

Table 5 shows the effect of colloidal $CaCO_3$ in static tests. The weight gain in this table is the weight of $CaCO_3$ coating deposited on stainless steel specimens. The weight loss is the metal lost after cleaning the corrosion products from cast iron specimens with an electric eraser. Less weight loss for cast iron specimens and more coating of stainless steel specimens resulted in tests where the water contained $CaCO_3$ in colloidal form than when colloids were absent, all other factors being the same.

It would seem that the development of good anti-corrosion protection requires an initial deposit of dense material which is well bonded to the metal. This layer need be but a few molecules thick. Upon such a foundation a hard and tenacious coating can then be developed. It has appeared that such initial layer should be of an adhering mixture of corrosion products and calcium carbonate. Neither rust alone nor calcium carbonate alone possesses the desirable

Table 5
Effect of Colloidal $CaCO_3$ for
Some Static Tests

Static test no. (from Table 1)	Sample	Weight increase due to formation of coating -- gms.	Weight loss after cleaning of corrosion products -- gms.
6*	Cast iron		0.1952
5	Cast iron		0.2264
9*	Cast iron		.2685
8	Cast iron		.3637
19*	Stainless steel cathode	.0550	
18	Stainless steel cathode	.0048	
19*	Stainless steel anode	.0059	
18	Stainless steel anode	.0004	
21+	Stainless steel cathode	.0007	
20	Stainless steel cathode	.0005	
21+	Stainless steel anode	.0012	
20	Stainless steel anode	.0003	

* Colloidal $CaCO_3$ present
+ Crystalline $CaCO_3$ present

qualities of the mixture. Rust not containing $CaCO_3$ has been too porous and not sufficiently dense. Pure calcium carbonate layers, on the other hand, were soft.

In the presence of $CaCO_3$ colloids the test waters were observed to move rapidly toward equilibrium. It is well recognized that calcium carbonate remains in supersaturated solution for long periods of time unless the reaction rate of calcium and carbonate ions in forming calcium carbonate is increased by the presence of crystal nuclei or by energy in the form of turbulence, high velocity or heat. The action of the colloidal calcium carbonate has been to accelerate the movement of the supersaturated solution toward equilibrium. Rapid deposition of calcium carbonate has resulted in the formation of an initial dense layer of the mixture, described above, before corrosion products had time to build up on the surface of the metal.

The positive charges of colloidal particles also aided the formation of the dense, hard coatings. These particles, due to their charges, were selectively laid down on cathodic areas of the metal surface through electrodeposition. As shown in polarization studies, it has been established that calcium carbonate acted as a cathodic inhibitor. The rate of corrosion thus was decreased because this cathodic film formation increased the polarization of cathodes in the corrosion cells on the surface of the metal.

It can be concluded from the above discussion that, due to selectivity in deposition, the over-all rate of corrosion was less in the presence of colloids than without such colloids, all other factors being the same. This finding was substantiated from weight loss determinations in Table 5.

With a decreased corrosion rate, calcium carbonate could interact with corrosion products in forming protective layers of the coatings. The formation of protective films on cathodic areas of the metal probably caused the formation of differential-aeration cells with the shielded cathodes becoming the anodes of the new cells. Thus mixtures of corrosion products and calcium carbonate would be deposited uniformly through the entire surface of the metal.

Figure 16 shows potential-time curves for Dynamic Tests 4 and 5. Colloidal $CaCO_3$ was the only variable, all other factors being the same; Test Water 5 contained $CaCO_3$ in colloidal form while no such colloids were present in Test 4. Corrosion potentials were measured against the saturated reference calomel electrode at the end of desired intervals of time.

The variation of potential with time during corrosion provided information of interest. Such potential variation serves to distinguish between the tendency to develop corrosion and the tendency to stifle corrosion. A continuously

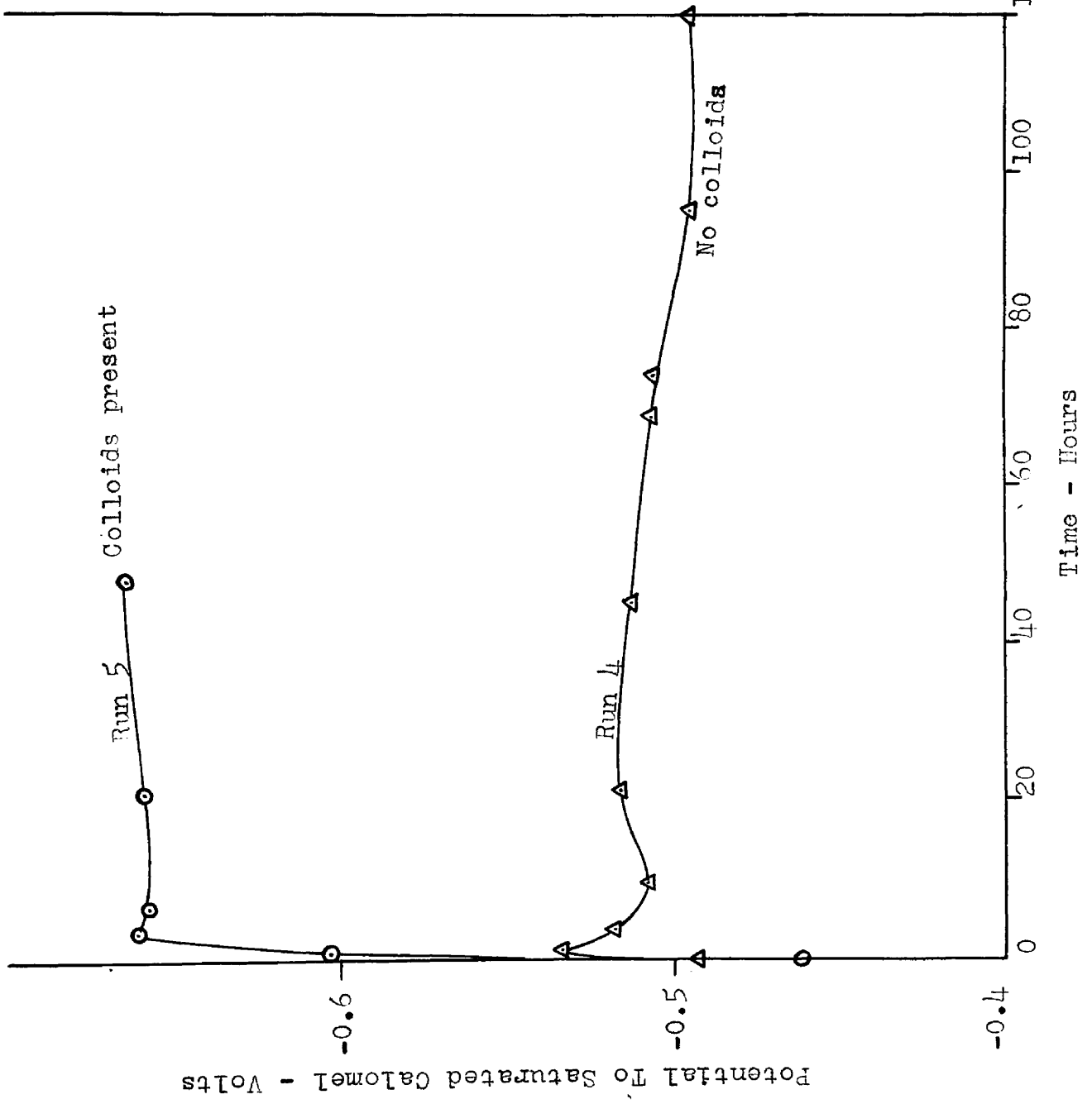

Figure 16 - Effect of Colloidal $CaCO_3$ on Coatings Developed

falling potential shows that the liquid is corrosive, while a steady or rising potential is noted when the liquid favors passivity. The absolute level of potential is without significance; interest attaches only to the question of whether potential rises or falls. It is to be recalled that when passivity is due to increased polarization of the cathode the resulting corrosion potentials are of less noble values (higher negative values) as compared to a standard calomel electrode.

With the absence of colloids in Run 4, the corrosion potential of cast iron specimen changed sharply to a less noble potential in the first hour. This initial change was followed by a rather sharp and gradual shift in the noble direction over the remainder period of 120 hours. The increase in negative value of the potential during the first hour can be attributed to the formation of corrosion products on the surface of the specimen. The subsequent decrease in potential values is probably due to removal of corrosion products from the surface of the specimen as the run was continued.

The corrosion potential of Test 5 where colloids were present shows a rapid shift in a less noble direction, followed by a steady and gradual shift in the same direction for the rest of 48 hours period. This shift indicated that the degree of passivity formed on cast iron specimen at the

beginning of the test was greater than for Run 4. Passivity was maintained and increased for the remaining period of the test.

It is to be noted that $CaCO_3$ crystals of larger than colloidal size did not have as favorable an effect on formation of coating, as colloidal $CaCO_3$. These crystals showed a typical calcite form under a microscope and carried no electrical charge.

The Effect of Momentary Excess on Coating Development

In an aqueous solution, the calcium and carbonate ions present which are in excess of the solubility product constant of calcium carbonate have been defined by Dye (32) as the "momentary excess." Momentary excess is invariably less than "saturation excess," which is the amount of calcium carbonate precipitation that must take place to bring a calcium-carbonate-bicarbonate-carbon dioxide system to equilibrium.

Since the concentration of carbonate ions in a given solution is a function of the pH level of that solution, high momentary excess values result from high pH levels. Low pH levels, conversely, produce low momentary excess values. The momentary excess level represents the driving force tending toward calcium carbonate deposition. Some

relationship, therefore, should exist between this excess and the rate of calcite deposition.

Table 6 shows values of momentary excess and saturation excess for waters which were studied in dynamic tests. In all tests shown the water contained calcium carbonate colloids. Tests were run for the period of time required to produce a definite coating, commonly one to five days.

Tests 7 and 8 were made at high pH levels (high momentary excesses). The coating on Test Specimen 7 was soft limonite covered by heavy, loose grained, and chalky deposits of calcite. It was apparent that there was no intermixing between limonite and calcite, especially in the layers closest to the metal. The coating of Test 8 consisted almost entirely of soft limonite, very little calcite being present. The rate of deposition of $CaCO_3$ was very high in these two tests. However, only a small part of the material was deposited on the test specimen, the remainder plating out at the bottom of the barrel reservoir and in the Tygon tubing of the apparatus.

Momentary excess values for the other tests of Table 6, were of much lower order than for the first two high pH studies. Hard, dense coatings were developed on all specimens with good to excellent bond to the metal. Calcite grains found in the coatings of these tests were of about half the size of those found at high pH levels. Uniform

Table 6
Relationship Between Saturation Excess, Momentary Excess, and Type of Coating Developed in Dynamic Tests

Test no.	pH	Hardness ppm $CaCO_3$	Saturation excess	Momentary excess	Relative protective value of coating developed
	10.25	83	66.5	46.5	7 (poorest coating)
	10.25	65	48.5	34.7	
9	8.6	150	30.0	5.4	
10	88.7	120	22.0	5.1	5
11	8.4	205	44.0	5.0	2
12	8.3	200	44.0	4.0	1 (best coating)
5*	8.6	92	14.5	2.7	3

* Colloids developed by raising pH above 10.0, then adjusting with CO_2.

intermixing of calcite and corrosion products generally appeared in all the tests with low momentary excess values.

Figure 17 shows the corrosion potentials of the specimens during some of the tests shown in Table 6. Potential values for Tests 7 and 8 of high pH levels and high momentary excess do not indicate a high level of passivity as compared to those of Tests 11 and 12 of low pH levels.

The relative protective values of coatings developed on cast iron specimens in static tests in the presence of $CaCO_3$ colloids is shown in Table 7 for different levels of momentary excess. This evaluation is also based upon hardness and bonding to metal.

Coating on the specimen from Test 13, which was conducted at a high momentary excess level of 46.5, was the poorest. This Test 13 coating was made of soft blotches of limonite with very little calcite. In Test 9 a low momentary excess value of 0.42 also produced a poor coating consisting largely of soft blotches and aggregates of limonite and siderite.

At a momentary excess level of 11.1 in Test 19, the coating obtained was made of calcite distributed between blotches of limonite and siderite. The limonite appeared to be relatively harder than that formed on specimens of Tests 11 and 13. Similar arrangement of calcite deposition between blotches of limonite and siderite was also obtained

Figure 17 - Corrosion Potentials at Different "Momentary Excess" Values

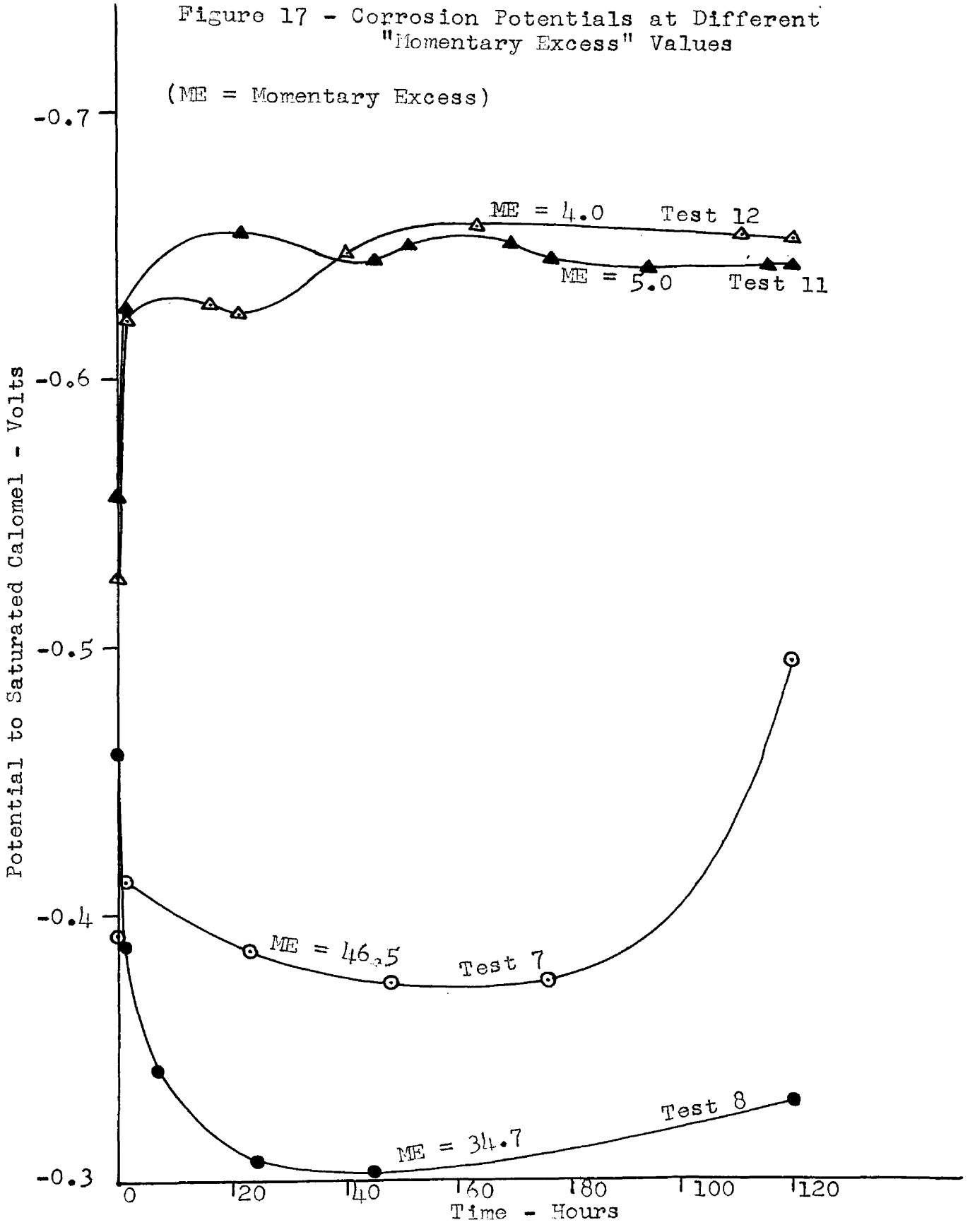

Table 7
Relationship Between Momentary Excess Levels and Type of Coating Developed on Cast Iron Specimens in Static Tests

Test no.	pH	Hardness ppm $CaCO_3$	Momentary excess	Relative protective value of coating developed
13	10.25	83	46.5	4 (poorest coating)
11	9.0	92	11.1	2
6*	8.6	92	2.7	1 (best coating)
9*	8.6	50	0.4	3

* Colloids developed by raising pH above 10, then adjusting with CO_2.

on specimen of Test 6. The blotches, however, were smaller in size than those formed on the specimen of Test 11, and the coating appeared slightly harder than that obtained in Test 11.

The same evaluation is shown in Table 8 for stainless steel specimens in static tests under different momentary excess levels. In these tests, the specimens were under a uniform applied current density of 1.034 ma/dm^2, and colloidal $CaCO_3$ was present in the test waters. The weight of $CaCO_3$ deposited on the cathodes and anodes of stainless steel specimens after a period of seven days is used as an index of the effect of momentary excess level.

Once again, coatings on specimens obtained from tests with high levels of momentary excess were the poorest, based upon hardness and bonding to metal. Better coatings developed in the tests with lower levels of momentary excess.

No relationship could be obtained between the weight of $CaCO_3$ deposited on the anodes and cathodes of stainless steel specimens and momentary excess levels. The data indicate, however, that the weight deposited on the specimens was more nearly related to hardness than to momentary excess. Generally the higher the level of hardness the more $CaCO_3$ deposited on both the cathode and anode of stainless steel specimens.

Table 8
Relationship Between Momentary Excess Levels, Type of Coating Developed, and Weight of $CaCO_3$ Coatings Deposited on Stainless Steel Specimens in Static Tests

Test no.	pH	Hardness ppm $CaCO_3$	Momentary excess	Relative protective value of coating developed	Weight of $CaCO_3$ deposited on the cathode (gm)	Weight of $CaCO_3$ deposited on the anode (gm)
27	10.25	83	46.5	4 (poorest coating)	0.0359	0.0152
26	9.5	100	22.1		0.0600	0.0209
25	9.1	150	17.1	3	0.0347	0.0165
24	9.5	70	14.9		0.0582	0.0013
23	8.8	240	14.8	1 (best coating)	0.1011	0.0459
22	9.1	100	10.2		0.0647	0.0185

From the above analyses of the relationship between momentary excess levels and the coating developed in both dynamic and static tests, it was considered that the anti-corrosion value of these coatings was, generally, in inverse ratio to momentary excess levels. That is, low momentary excess levels produced superior type coatings.

Low momentary excess levels with high saturation excess values, in the presence of $CaCO_3$ colloids, led to the formation of the best coating developed, especially in dynamic tests. These coatings were tenacious, hard and protective. This combination of low momentary excess and high saturation excess occurs when the test water is in the pH range of 8.2 to 8.7 and has a momentary excess between 2.5 and 5.5. Levels of pH higher than 9.5 were definitely established as undesirable.

Effect of the Age of Colloidal Particles On the Rate of Deposition of $CaCO_3$ and Coating Development

It was found that the rate of deposition of $CaCO_3$ from supersaturated solutions containing colloidal material was not only related to the momentary excess levels of the solutions but also to the age of the colloidal material present.

Three identical Dynamic Tests 14, 15, and 16 were made

with the same testing water at pH of 8.3 and momentary excess value of 4.0. Test 15 was made four days after Test 14 while Test 16 was made twenty days after Test 14. The only difference between the tests lay in the age of the colloidal material in suspension. Precipitation in Test 14 was 15 ppm per day, in Test 15 was 45 ppm per day, and in Test 16 was 60 ppm in six hours.

Both Tests 14 and 15 produced good protective coatings in one day's time. The coating of the Test 14 specimen was of smoother texture and did not show the very marked ridges and valleys of the specimen's coating of Test 15. The coating of Test 15 seemed slightly harder and better bonded to the metal surface.

Figure 18 shows corrosion potential-time curves for Tests 14 and 15. The figure indicates that the passivity acquired by the specimen of Test 15 was still increasing at the end of one day's time, while that of Test 14 had reached an almost steady level by the end of a half-hour period.

Coatings from Test 16, where the rate of precipitation was high (60 ppm in 6 hours), were checked at the end of six hours and found to be very poor. The coating could be removed easily by a finger nail as the limonite was very soft. Analyses indicated that percentage calcite in the coating was much less than that of Tests 14 and 15, although the rate of deposition of $CaCO_3$ was much higher.

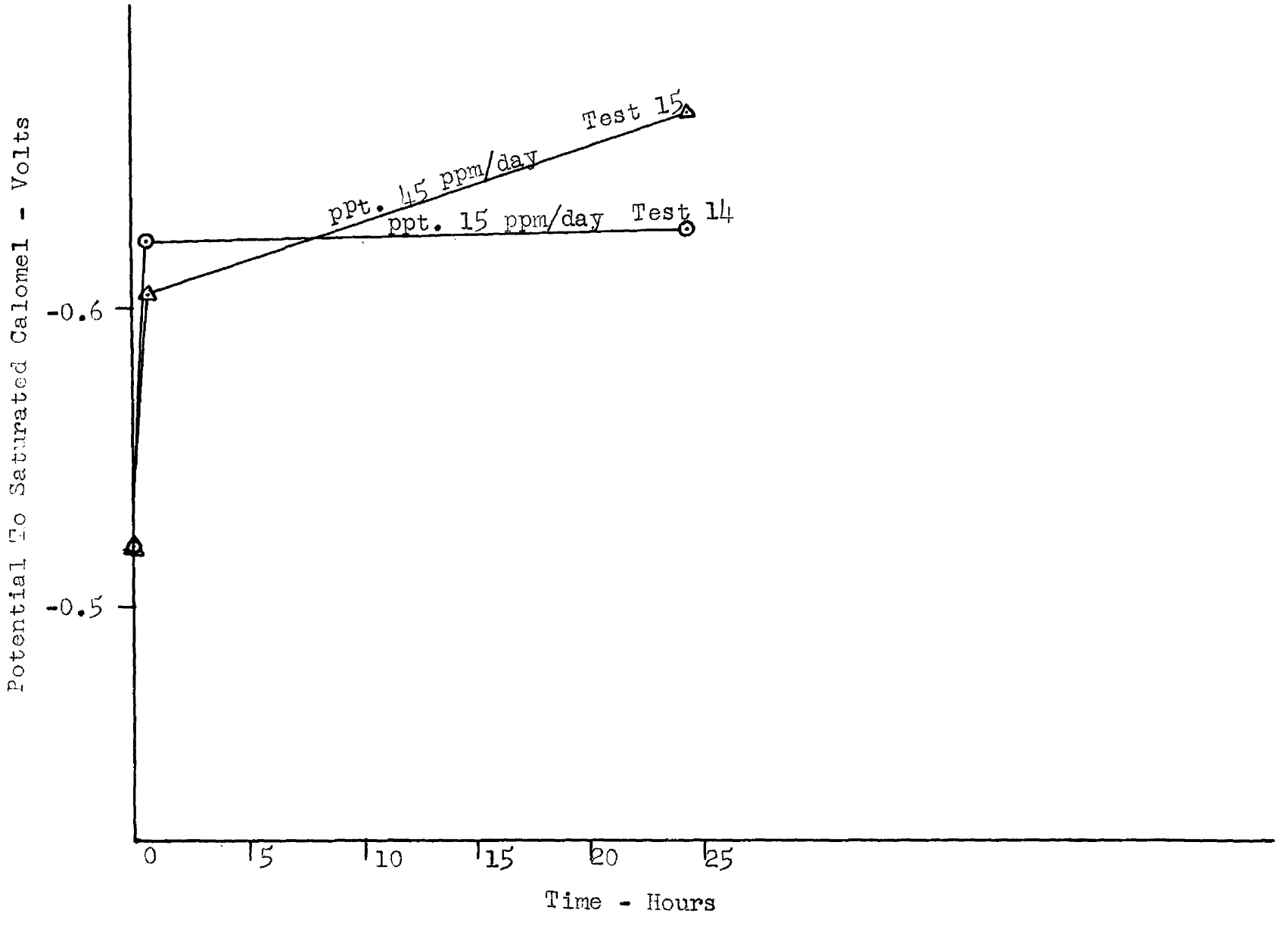

Figure 18 - Effect of Rate of Deposition of $CaCO_3$ on Coatings Developed

The effect of the age of colloids on the rate of deposition of $CaCO_3$ and consequently on the coatings developed can also be shown in Dynamic Tests 12 and 13. These two tests were also conducted at pH of 8.3 and momentary excess value of 4.0. Test 13 was made 7 days after the beginning of Test 12, using the same testing water. The average precipitation in Test 12 was 10.2 ppm per day and that of Test 13 was 52.5 ppm per day.

Coatings developed on the specimens at the end of five days with Test 12 and four days with Test 13 were both good, dense, and hard, with good bonding to the metal. However, the coating of Test 12, was of smoother texture, somewhat harder and better bonded to the metal than that of Test 13.

Potential-time curves for Tests 12 and 13 are shown in Figure 19. Specimen potential of Test 13, where the rate of deposition of $CaCO_3$ was higher, shifted more rapidly to large negative values at the beginning of the tests than for the specimen of Test 12. As the tests progressed, the specimen of Test 12 acquired more protection than that of Test 13.

It was evident from these and other tests that the rate of deposition of calcium carbonate had very significant influence on the type of coatings developed. Good coatings were produced only under a certain range of deposition rates. Below or above that range coatings were

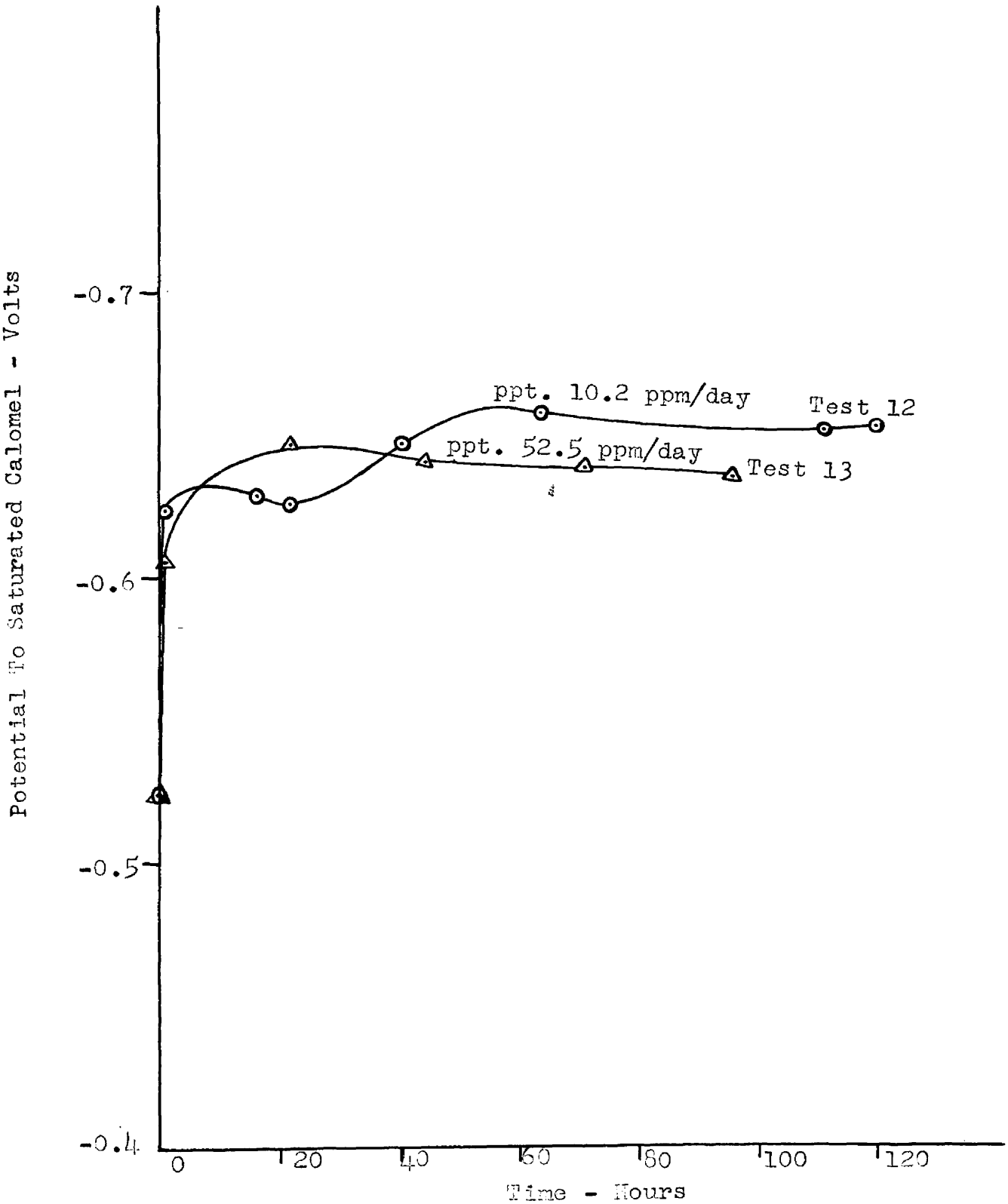

Figure 19 - Effect of Rate of Deposition of $CaCO_3$ on Coating Developed

poor. This optimum range of deposition rate was achieved when the test water was within the range of pH and momentary excess levels recommended in the discussion on the influence of momentary excess levels and when the colloids were newly formed.

As colloids became older and probably larger in size, the rate of deposition of $CaCO_3$ increased although the test water was maintained at the same levels of pH and momentary excess. In Test 16, the rate of deposition increased beyond the limited range recommended and resulted in a poor coating.

Effect of Dissolved Oxygen Levels on Coatings Developed

Levels of dissolved oxygen other than for saturation were studied in Dynamic Tests 17, 18, 19, 20, 21, 22 and 24. Table 9 shows dissolved oxygen levels for these studies. Analysis of the coatings developed is also shown in Table 9.

Test waters for Dynamic Tests 20, 21, 22 and 24 were identical; the pH level was 8.3, hardness was 180 ppm and colloidal $CaCO_3$ was present. Dissolved oxygen level was the only variable in these four tests.

The coating developed at low dissolved oxygen level of 0.88 to 2.1 ppm in Test 20 was soft and flaky, chiefly (79%) limonite. The percent calcite was relatively low. Very

Table 9
Effect of Dissolved Oxygen on Coatings Developed

Dynamic test no.	pH	Hardness	Dissolved oxygen ppm	Duration of the test	% $CaCO_3$	% $FeCO_3$	% $FeO(OH)$	% Fe_3O_4
17	10.25	65	1.5 - 2.5	5	10	5	20	65
18	8.3	200	1.7 - 2.7	4	30	20	50	0
19	8.3	200	27 - 28	3	20	15	63	2
20	8.3	180	0.88 - 2.1	3	10	10	79	1
21	8.3	180	4.0 - 5.0	3	25	15	59	1
22	8.3	180	7.0 - 8.0	3	25	20	54	1
24	8.3	180	10.0 - 11.0	3	10	10	79	1

small amounts of limonite, siderite and magnetite were found next to the metal, which was covered by a smooth soft layer of calcite. There was no tendency toward the linear arrangement that usually characterized dynamic runs at a saturated level of dissolved oxygen. It was quite apparent that there was no intermixing of calcite and corrosion products.

Evan (14) has stated that calcium carbonate in the presence of sufficient oxygen will interact with iron salts formed below to give a clinging form of ferric oxide rust. This mixed layer will be more protective if oxygen is present in large amount because the oxidation of ferrous compounds, which form first, is sufficiently rapid to ensure that hydrated ferric oxide is precipitated next to the metal. At low oxygen concentration the rate of oxidation of ferrous hydroxide to ferric hydroxide is slow enough to permit precipitation of both ferrous and ferric hydroxides with subsequent formation of magnetite out of physical contact with the metal.

In Test 20 only one percent of magnetite was found in the coating. Calcium carbonate was probably laid down before sufficient hydrated ferric oxide precipitated next to metal to permit intermixing with calcite.

The coating obtained at a higher dissolved oxygen level of 4 - 5 ppm on the specimen of Test 21 revealed quite different characteristics as compared to those noted on the

specimen of Test 20. Linear arrangement of ridges and valleys was clearly shown. A larger amount of corrosion products was formed in the coating. Although most of the calcite present was on the top of the coating, petrographic examination showed some intermixing with the products of corrosion near the metal surface. The coating was soft and could be removed easily with a finger nail. The rate of oxidation of ferrous hydroxide and subsequent precipitation of ferric hydroxide next to the metal was apparently still not sufficient to allow thorough intermixing with calcium carbonate.

A harder and better coating was obtained in Test 22 where the test water was saturated with dissolved oxygen (7 - 8 ppm). The linear arrangement was more pronounced than for Test 21. The most prominent quality distinguishing the coating from those obtained at lower dissolved oxygen levels was the thorough intermixing of calcite with corrosion products.

Test 24 was conducted at a dissolved oxygen level higher than saturation, in the 10 - 11 ppm range. An irregular, uneven, blotchy coating resulted in this study. Relatively hard blotches of limonite, siderite, and magnetite overlaid by calcite covered a portion of the surface of the specimen. The rest of the surface was clean metal with no coating.

The mechanism of formation of this coating, apparently, was different from that in effect at dissolved oxygen levels below saturation. The rate of precipitation of ferric hydroxide next to the metal surface probably was too fast to permit intermixing with calcite near the metal.

Figure 20 shows potential-time curves for Tests 20, 21, 22 and 24. The curve of Test 20, which was studied at the lowest oxygen level of 0.88 - 2.1 ppm, indicates formation of a temporary passivity at the beginning of the test. This passivity was probably due to the precipitation of a loose mixture of ferrous hydroxide, ferric hydroxide and magnetite which was removed as the test progressed.

As dissolved oxygen levels increased in Tests 21 and 22, potential-time curves indicate that the passivity formed at the beginning of the tests, due to formation of ferric hydroxide, acquired more permanent form. Specimen potential of Test 24, which was conducted at an oxygen level of 10 - 11 ppm, shifted very sharply to high negative values at the beginning of the test. This rapid shifting was followed by rapid falling and then by a slower steady fall. The sharp rise of potential at the beginning of Test 24 can be attributed to the excess deposition of loose ferric hydroxide, which was then removed from the surface of the metal as the test progressed.

Test 17 was studied at low oxygen level of 1.5 - 2.5

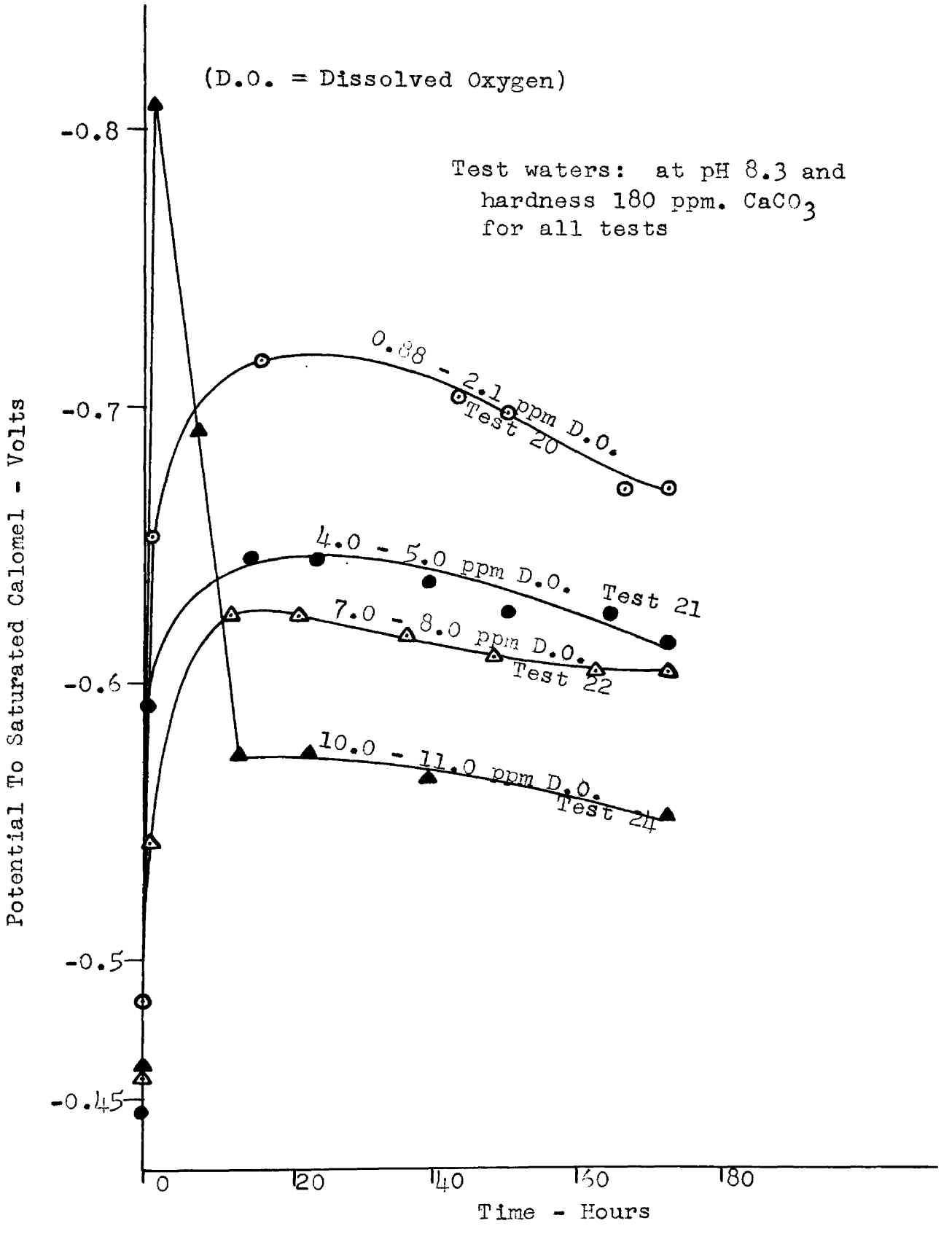

Figure 20 - Effect of Dissolved Oxygen Levels on Coatings Developed

ppm and high momentary excess value of 34.7 with a high rate of $CaCO_3$ deposition. The test water was at a pH of 10.25, and a hardness of 65 ppm, and contained $CaCO_3$ colloids. The resulting coating was uneven and irregular, consisting mostly of magnetite, and covering a large part of the specimen surface.

Sixty five percent of the specimen coating obtained from Test 17 was black magnetite. The insufficient supply of oxygen and high rate of $CaCO_3$ deposition prevented further oxidation of ferrous hydroxide which precipitated with ferric hydroxide on the metal surface. Interaction of ferric and ferric hydroxides thus yielded magnetite. The coating contained a relatively small percentage of calcite after 5 days. $CaCO_3$ apparently was removed as the test progressed due to poor bonding to either iron oxides or to the metal surface.

The potential-time curve of Test 17 is shown in Figure 21. The curve indicates that the cast iron specimen began to acquire some passivity only after about 40 hours had elapsed. This passivity may be attributed to precipitation of sufficient ferric hydroxide to allow some intermixing with calcite at this stage of the test. Formation of large amounts of magnetite which appeared to be somewhat hard may also have contributed to this passivity.

Test 18 was conducted at a pH of 8.3, a hardness of

Figure 21 - Effect of Dissolved Oxygen Levels on Coatings Developed

(D.O. = Dissolved Oxygen)

Test water 17: pH 10.25, hardness 65 ppm

Test water 18: pH 8.3, hardness 200 ppm

Test water 19: pH 8.3, hardness 200 ppm

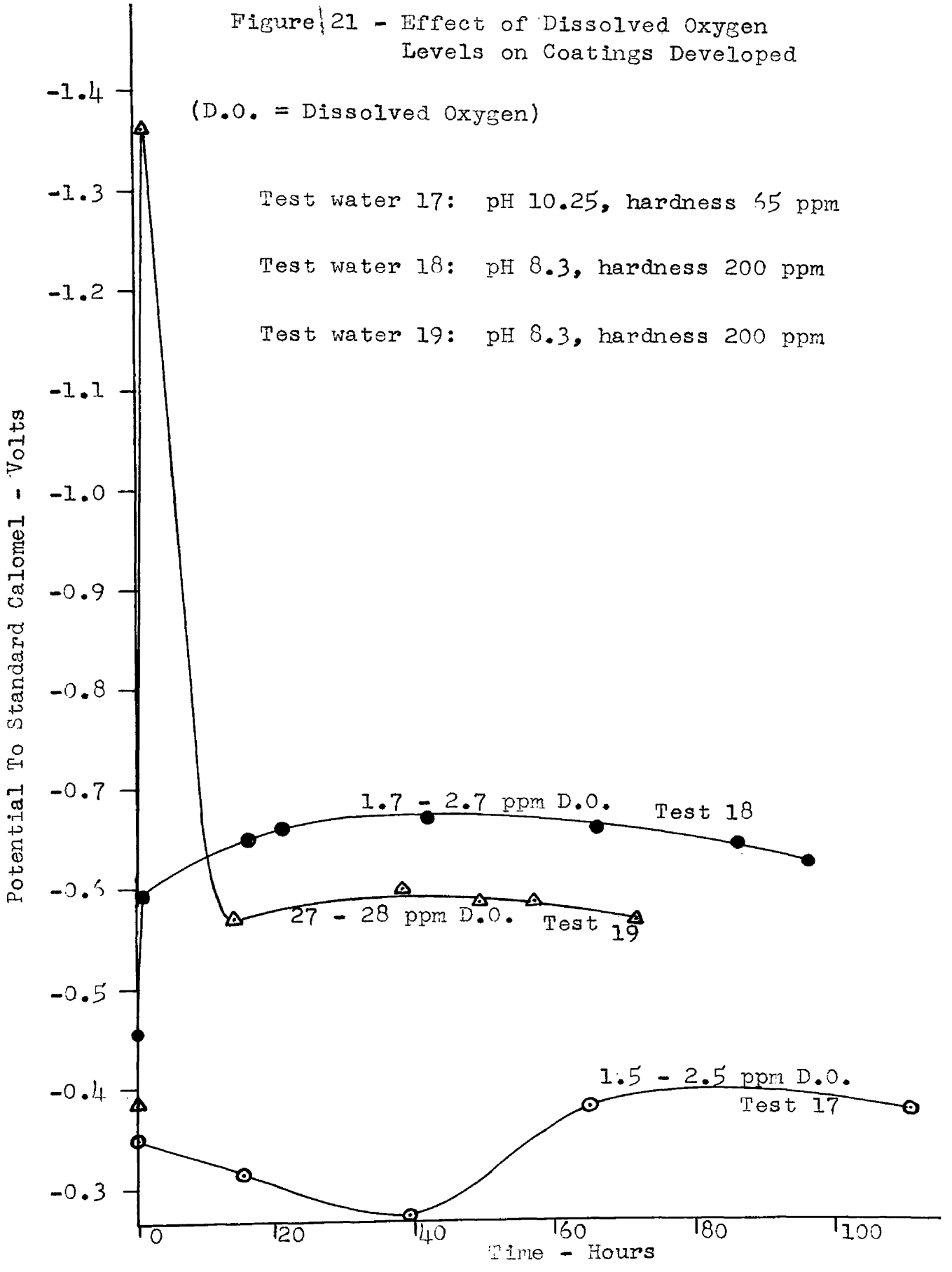

200 ppm, a dissolved oxygen level of 1.7 - 2.7 ppm, and in the presence of $CaCO_3$ colloids. After four days the coating was soft and similar to that obtained from Test 21. A heavy calcite layer overlaid the coating, while limonite and siderite were found next to the metal. Very little intermixing occurred between calcite and the products of corrosion. Potential-time curve of the specimen of this test, shown in Figure 21, indicates similar behavior to that of Test 21.

A very high level of dissolved oxygen was used in Test 19. This test was at a pH of 8.3, a hardness of 200 ppm, a dissolved oxygen level of 27 - 28 ppm, and in the presence of colloidal $CaCO_3$. A soft coating was obtained. An excess of corrosion products was observed near the metal surface covered by a calcite layer. Obviously, the deposition of ferric hydroxide near the metal surface was too fast to permit intermixing with calcite.

The distinguishing characteristic of the coating obtained from Test 19 and as compared with that obtained from Test 24 at an oxygen level of 10 - 11 ppm was one of uniformity. The coating of Test 19 covered the entire surface of the specimen while that of Test 24 covered only part of the metal surface.

Figure 21 shows the potential-time curve of Test 19. The general shape of the curve was similar to that for Test 24 shown in Figure 20. The rise and fall of potential

values at the beginning of Test 19 was greater than the corresponding shift of potential values in Test 24. This was probably due to greater precipitation of loose ferric hydroxide on the metal surface at the early stage of Test 19 and subsequent removal of these precipitates.

It can be concluded from the above discussion that in order to develop a good, hard, and uniform coating, a coordination should exist between the rate of deposition of $CaCO_3$ and the rate of formation and precipitation of ferric hydroxide next to the metal surface. At the rates of deposition of $CaCO_3$ studied, it appeared that saturation of test water with dissolved oxygen was the optimum level, permitting thorough intermixing of calcium carbonate and consequently resulting in the development of a favorable coating.

Effect of Specimen Surface Conditions on Coatings Developed

Two cast iron specimens were mounted in the test cell of the flow system of Test 11. One of the specimens was sand blasted while no surface conditioning was applied to the second specimen other than a standard procedure of surface grinding with a 40-grit diamond dressed wheel which was used for all cast iron specimens in the study. The

test was conducted at a pH of 8.4, a hardness of 205 ppm, saturation with dissolved oxygen, and in the presence of $CaCO_3$ colloids.

No difference in composition, hardness, or bonding to metal was noticed in the coatings developed on the two specimens. Potential-time curves revealed a slight difference in the passivity acquired by the two specimens, as shown in Figure 22. The sand blasted specimen curve shows slightly higher passivity than for the smooth metal, especially after about 80 hours had elapsed. Roughening the surface of the cast iron specimen probably helped the bonding of the coating to the metal surface to some degree.

Two identical dynamic Tests 12 and 13 were undertaken with identical test water; pH 8.3, hardness 200, saturated with dissolved oxygen, and containing colloidal $CaCO_3$. A sand blasted stainless steel specimen was used in Test 12 while Test 13 was conducted with a smooth surface stainless steel specimen.

No observable deposit formed on the smooth specimen after a period of four days and no significant deposit was noted on sand blasted specimen after five days. This absence of the formation of coatings on stainless steel specimens in flow system without applied EMF substantiated the work of Strum (16). Strum has reported that practically no $CaCO_3$ was precipitated at the surface of stainless steel surface

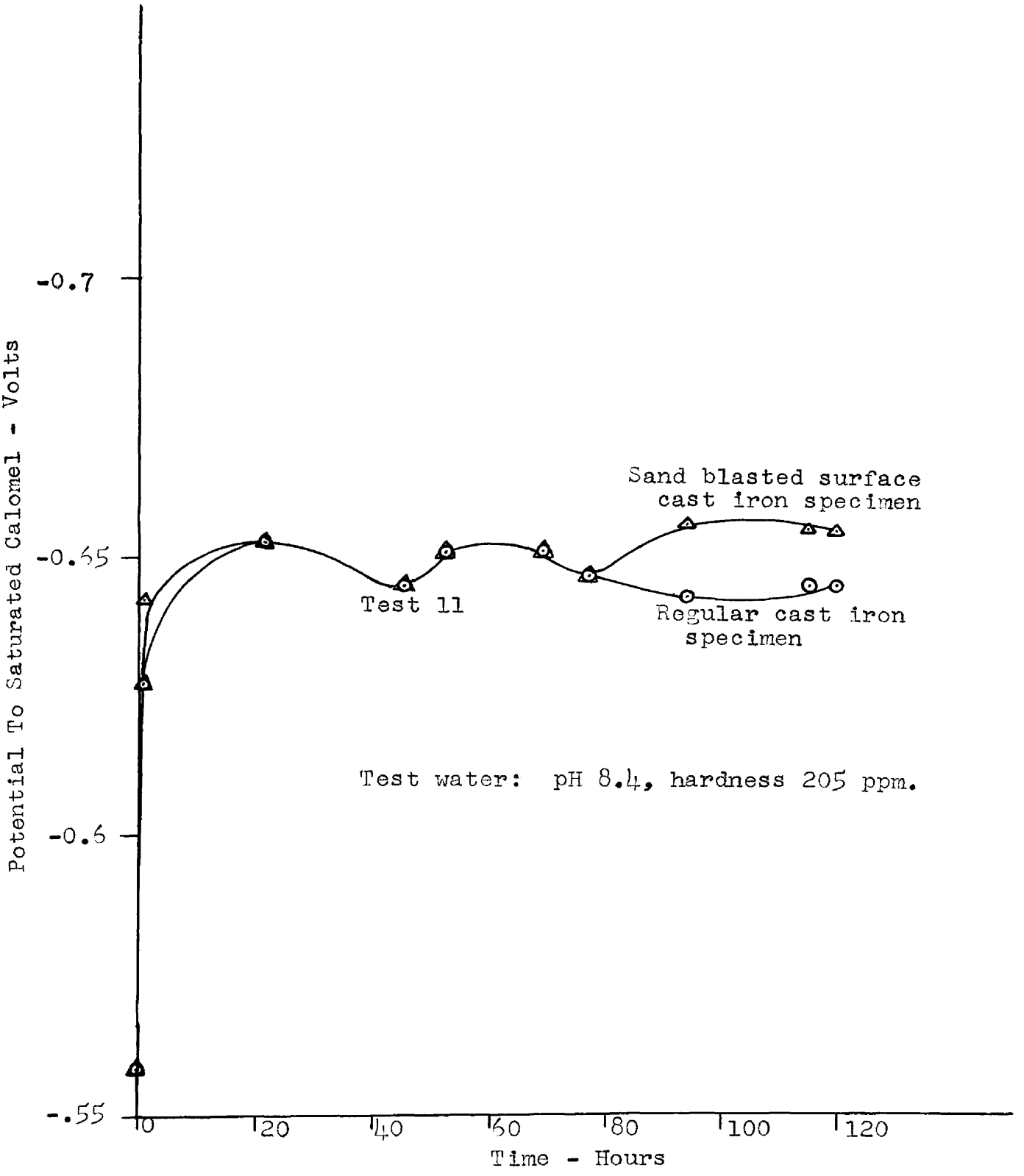

Figure 22 - Effect of Cast Iron Specimen Surface on Coatings Developed

in a five-day period even though the saturation index of the testing water was +1.05 pH unit.

Figure 23 shows potential-time curves for Tests 12 and 13. The figure indicates that the sand blasted specimen possessed relatively better passivity than the smooth surface specimen as the tests progressed. The roughness of the surface apparently helped to hold a very slight coating of $CaCO_3$ on the surface of the sand blasted specimen and thus caused the difference in passivity.

A coating of $CaCO_3$ on the sand blasted stainless steel specimen was obtained in Static Test 28 without an electric current being applied. This static test was conducted at pH 8.8, hardness of 220 ppm, and in the presence of $CaCO_3$ colloids. An uneven, hard coating covered a large portion of the surface of the specimen. Crystals and aggregates of calcite tended to build up on one another, especially around the pits of the sand blasted surface. The absence of a continuous flow of water and of the turbulence around the specimen in static tests created condition favorable to deposition and bonding of $CaCO_3$ to the rough surface of the sand blasted specimen.

The physical condition of metallic surface on cast iron specimens had much less influence upon coating development than the environmental conditions discussed earlier in the section. The deposition of calcium carbonate on cast iron

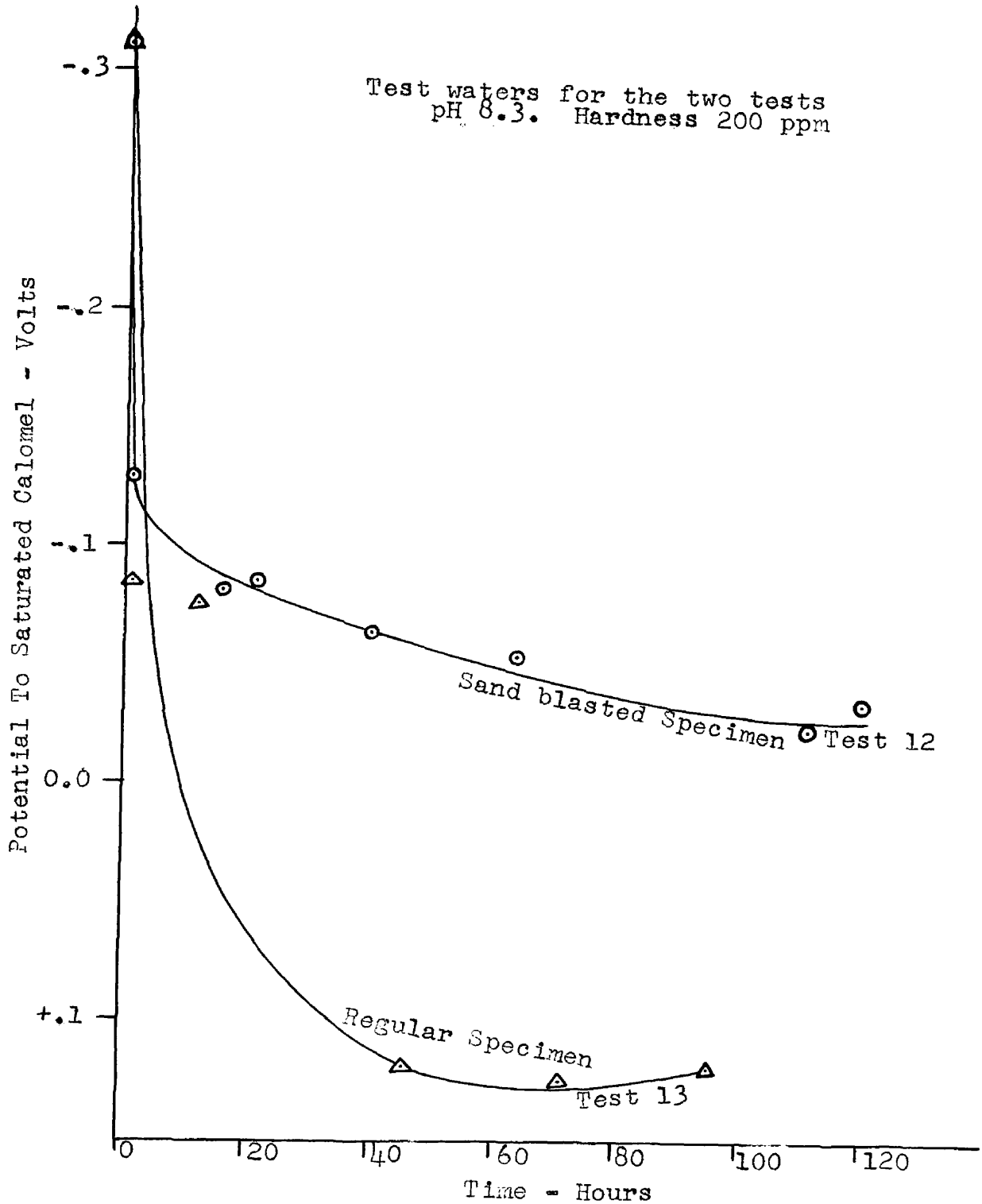

Figure 23 - Effect of Stainless Steel Specimen Surface on Coatings Developed

specimens and the lack of this deposition of stainless steel specimens in dynamic tests indicated the importance of corrosion products in the formation of the coatings on cast iron specimens.

Effect of Iron Oxide on Coating Development on Stainless Steel Specimens

Ferric oxide was prepared by adding 2% of ferric chloride solution to a large volume of hot water. The resulting solution was then allowed to boil until a positively charged colloid of iron oxide was obtained.

Stainless steel specimens were used in Static Test 29, which contained 3.2 ppm (as Fe) of this positively charged iron oxide colloid. Test 29 was conducted at pH 9.6, hardness of 90 ppm and in the presence of $CaCO_3$ colloids. No applied electric current was used.

It was observed that when colloidal ferric oxide was added to the test water at pH 9.6 large particles of iron oxide were formed, most of which precipitated quickly into the bottom of the glass cylinder. These particles carried no electric charge. The level of iron oxide was adjusted periodically in the same way as for the standard procedure for pH and hardness of test water.

Calcium carbonate coatings developed after a week's

time contained 1 - 2 percent iron oxide. The coating was harder and tougher than any other coating of $CaCO_3$ developed on stainless steel specimens in this study with or without applying electric current. This test showed clearly the effect of intermixing of $CaCO_3$ and iron oxide on the coating developed.

Dynamic Test 25 was conducted at pH 8.3, hardness 200 ppm, and in the presence of $CaCO_3$ colloids. One ppm of iron oxide colloid (as Fe) was added to the test water. A sand blasted stainless steel specimen was used. Iron oxide colloids acted in the same manner as in static Test 29, growing into large particles, most of which precipitated quickly. The level of iron oxide was adjusted periodically, as in the regular procedure for pH and hardness of test water. No applied electric current was used.

An uneven soft coating of $CaCO_3$ with 1 - 2 percent iron oxide was obtained after three day's period. Only part of the surface of the specimen was coated. Iron oxide was deposited close to $CaCO_3$ deposits.

It is to be recalled that it was not possible to obtain any observable coating of $CaCO_3$ on stainless steel specimens (with sand blasted and regular surfaces) in dynamic Tests 12 and 13 which were conducted under identical conditions of pH 8.3, hardness 200 ppm, and in the presence of $CaCO_3$ but with no iron oxide present.

Iron oxide, therefore, aided in the formation of the coating obtained in Test 25. The rate of deposition of $CaCO_3$ was relatively large due to the presence of iron oxide particles which aided the growth and precipitation of $CaCO_3$ colloids. Probably high rate of deposition of $CaCO_3$ with insufficient amount of iron oxide to interact with caused the formation of soft coating.

Static Tests VS. Dynamic Tests

Generally, coatings obtained from static tests were soft and poorly bonded to the metal. Coatings developed on cast iron specimens in the absence of $CaCO_3$ colloids were a mixture of calcium and ferrous carbonate and iron oxide, bonded to a porous layer of rust. In the presence of colloidal material, the coatings consisted of calcite distributed between blotches of limonite and siderite.

Better bonded, harder, and more uniform coatings generally were obtained in dynamic tests. A linear arrangement of ridges and valleys was the most prominent characteristic distinguishing dynamic tests from static tests. In most dynamic tests, calcite was found largely in the valleys while ridges were commonly limonite at the surface with siderite deposited below near the metal. Under favorable conditions, the ridges and valleys were built upon a uniform

layer of mixed calcite and corrosion products well bonded to the metal.

Ferric hydroxide requires oxygen for its precipitation. In dynamic tests under saturation condition, oxygen was in excess and uniformly available over the entire surface of the specimen. Ferric hydroxide, could then be precipitated very close to the metal in a uniform thin layer. Subsequent deposition of calcium carbonate uniformly over the entire surface would lead to thorough intermixing, resulting in a uniform protective coating.

In static tests, the source of oxygen was at a distance from the metal and the main site of precipitation of ferric hydroxide was not close to the metal surface. The precipitation was then concentrated on certain areas of the metal and blotchy coatings resulted from many static tests. In addition, the specimens did not show uniform deposition of $CaCO_3$ as in dynamic tests.

All dynamic tests studied were at a linear velocity of two feet per second. Since dynamic and static tests conducted under identical conditions produced two distinctive types of coatings it is obvious that velocity has significant influence on coating development.

CONCLUSIONS

The following conclusions are drawn from the investigations undertaken in this thesis:

1. Calcium carbonate acted primarily as a cathodic inhibitor.

2. The action of calcium carbonate in developing good protective coatings lay in its forming a physical mixture with corrosion products.

3. Coating materials developed on cast iron specimens were largely hydrous ferric oxide in the form of limonite. From 5 to 40 percent calcite was commonly present. Siderite and magnetite were usually observed, covered by limonite and calcite. With stainless steel specimens calcite alone formed the entire coating.

4. Better protection and better bonded, harder, and tougher coatings resulted from solutions containing colloidal $CaCO_3$ than from identical solutions of the same pH and hardness with no colloids present.

5. Colloidal $CaCO_3$ had a positive charge in the pH range of 6 to 11 and may be represented as $(CaCO_3)\ Ca^{++}\vdots O^{=}$.

6. $CaCO_3$ crystals in suspension did not have a favorable effect on formation of coatings from supersaturated

solutions.

7. A high "momentary excess" level of calcium carbonate led to the formation of chalky soft coatings. Low "momentary excess" and high "saturation excess" levels of $CaCO_3$ led to the formation of tenacious and hard, protective coatings.

8. Rate of deposition of $CaCO_3$ from supersaturated solutions containing colloidal material was influenced not only by the "momentary excess" value but also by the age of colloids present.

9. A dissolved oxygen level of saturation was optimum for development of good protective coatings under the conditions carried out in this study.

10. High velocity flow rates were desirable in the formation of hard and durable coatings. Static tests produced soft coatings.

11. Surface condition of cast iron specimens had little effect on the type of coatings developed.

12. It has been established from the investigations undertaken in this study that when the test water was saturated with dissolved oxygen, of pH range from 8.2 to 8.7, with "momentary excess" levels of 2.5 to 7.5, flow rate of about two feet per second, and containing colloidal $CaCO_3$, a uniform, dense, hard coating which was well bonded to the metal was developed on cast iron specimens in one day's time at room temperature.

RECOMMENDATIONS

It has been established that the presence of colloidal $CaCO_3$ in supersaturated solutions and the rate of deposition of $CaCO_3$ have an important effect on the type of coatings developed. Unfortunately, the rate of deposition of $CaCO_3$ was found to be not only a function of the "momentary excess" level of supersaturated solution but also of the age of colloidal particles present. It was apparent that the older and probably larger calcium carbonate colloids increased the rate of deposition. Stabilizing of these colloids would be very desirable. The rate of deposition of calcium carbonate could then be controlled by the level of "momentary excess" alone.

A flow of two feet per second velocity was found desirable in producing hard protective coatings as compared to static conditions which produced soft coatings. Only one level of flow rate, two feet per second, was studied throughout all dynamic tests. Investigations of the effect of other flow rates might prove beneficial in producing hard durable coatings.

In order that the conditions of the tests conducted in this study parallel the conditions normally encountered in water distribution systems

normally found in a water distribution system, on coatings developed should be investigated under the general conditions recommended in this study for producing good protective coatings.

Judgment of coatings upon the basis of bond to the cast iron, hardness, and toughness has been reasonably satisfactory for these studies but a better method for evaluation is desirable.

BIBLIOGRAPHY

(1) Johnson, J., Merwin, H.F., and William, E.D., "The Several Forms of Calcium Carbonate," Am. J. of Sci., 4th Series 41: 473 (1916).

(2) Tillmans, J., "Die Chemische Untersuchung Von Wasser," Verlog von Wilhelm Knapp, Soale, Ger. (1936).

(3) Langelier, W.F., "The Analytical Control of Anti-Corrosion Water Treatment," J. Am. Water Works Assoc., 28: 1500 (1936).

(4) Moore, E.W., "Calculation of Chemical Dosages Required for the Prevention of Corrosion," J. New Engl. Water Works Assoc., Sept.: 311 (1938).

(5) Enslow, L.H., "The Continuous Stability Indicator," Water Works & Sewage, 86: 169 (1946).

(6) Langelier, W.F., "Chemical Equilibria in Water Treatment," J. Am. Water Works Assoc., 38: 169 (1946).

(7) McKinney, D.S., "The Calculation of Equilibria in Dilute Water Solutions," Proc. Am. Soc. Testing Materials, 39: 1191 (1939).

(8) Larson, T.E., and Buswell, A.M., "Calculation of Calcium Carbonate Saturation Index and Alkalinity Interpretations," J. Am. Water Works Assoc., 34: 1667 (1942).

(9) Ryznar, J.W., "A New Index for Determining Amount of Calcium Carbonate Scale Formed by a Water," J. Am. Water Works Assoc., 36: 472 (1944).

(10) Dye, J.F., "The Calculation of Alkalinity and Free Carbon Dioxide in Water by the Use of Nomographs," J. Am. Water Works Assoc., 36: 893 (1944).

(11) Larson, T.E., and King, R.M., "Corrosion by Water at Low-Flow Velocity," J. Am. Water Works Assoc., 46: 1 (1954).

(12) Raistrick, B., "Condensed Phosphate and Corrosion Control," Chem. & Ind. No. 19: 408 (1952).

(13) Evan, U.R., "The Practical Problems of Corrosion," J. Soc. Chem. Ind., 47: 55 (1928).

(14) Evan, U.R., "Metallic Corrosion, Passivity, and Protection," Edward Arnold Pub. Co., London (1937).

(15) Haase, L.W., Deposits and Protective Coatings," Werkstoffe u. Korrosion, 5: 198 (1952).

(16) Strum, W., "Calcium Carbonate Deposits," J. Am. Water Works Assoc., 48: 310 (1956).

(17) Baylis, J.R., "Factors Other than Dissolved Oxygen Influencing the Corrosion of Iron Pipes," Ind. Eng. & Chem., 18: 370 (1926).

(18) Schikorr, G., "The Breakdown of Metals," Barth, Leipzig (1943).

(19) Haupt, H., "Protection of Pipes by Removal of Acids From Portable Waters," Gesundh. Ing., 64: 333 (1941).

(20) Camp, T.R., "Corrosiveness of Water to Metals," J. New Engl. Water Works Assoc., June: 188 (1953).

(21) Schikorr, G., "Iron Hydroxides Formed in Rusting," Anorg. Chem., 191: 322 (1930).

(22) Girard, A., "A Detailed Study of Formation of the Different Forms of Rust," Thesis, Lille, (1937).

(23) Whitney, W.R., "The Corrosion of Iron," J. Am. Chem. Soc., 25: 394 (1903).

(24) Uhlig, H.H., ed., "Corrosion Handbook," John [illegible] Sons, New York (19[illegible]).

(25) Speller, F.N., "Corrosion, Causes and Prevention," McGraw-Hill Book Co., New York (3rd ed., 1951).

(26) Eliassen, R., and Lamb, J.C., "Mechanism of the Internal Corrosion of Water Pipe," J. Am. Water Works Assoc., 45: 1281 (1953).

(27) Hadley, R.F., "Microbiological Anaerobic Corrosion," Am. Gas Assoc. Proc., 22: 764 (1940).

(28) Wilson, R.E., "The Mechanism of the Corrosion of Iron and Steel in Natural Waters and the Calculation of Specific Rates of Corrosion," Ind. Eng. & Chem., 15: 127 (1923).

(29) Powell, S.T., Bacon, H.E., and Lill, J.R., "Corrosion Prevention by Controlled Calcium Carbonate Scale," Ind. Eng. & Chem., 37: 942 (1945).

(30) Dye, J.F., "Calculation of Effect of Temperature on pH, Free Carbon Dioxide and the Three Forms of Alkalinity," J. Am. Water Works Assoc., 44: 351 (1952).

(31) Hoover, C.P., "Stabilization of Lime-Softened Water," J. Am. Water Works Assoc., 34: 1425 (1942).

(32) Dye, J.F., Private Communication.

(33) HachVer Catalog, Hach Chemical Co., Ames, Iowa, Catalog No. 3.

(34) "Standard Methods for the Examination of Water, Sewage, and Industrial Wastes," American Public Health Association, Inc., (10th ed., 1955)

(35) Von Weimarn, P.P., "The Colloidal, Amorphous, and Crystalline States of Matter," Z. Chem. Ind. Kolloid, 2: 76 (1907).

(36) Larson, T.E., and Buswell, A.M., "Water Softening," Ind. Eng. & Chem., 32: 132 (1940).